



Utrecht University
Faculty of Geosciences

**Living deep-sea benthic foraminifera from
the Cap de Creus Canyon (western
Mediterranean): faunal-geochemical
interactions**

by

Lorena Astrid Contreras Rosales

Supervisors:

Dr. Karoliina Koho

Utrecht University, Department of Earth Sciences

Dr. Ivo Duijnste

Utrecht University, Department of Earth Sciences

Dr. Henko de Stigter

Royal Netherlands Institute for Sea Research

Dr. Lucas Lourens

Utrecht University, Department of Earth Sciences

Master Thesis

August 2010

Utrecht University
Faculty of Geosciences

Living deep-sea benthic foraminifera from the Cap de Creus Canyon (western Mediterranean): faunal-geochemical interactions

by

Lorena Astrid Contreras Rosales

Supervisors:

Dr. Karoliina Koho

Utrecht University, Department of Earth Sciences

Dr. Ivo Duijnstee

Utrecht University, Department of Earth Sciences

Dr. Henko de Stigter

Royal Netherlands Institute for Sea Research

Dr. Lucas Lourens

Utrecht University, Department of Earth Sciences

With data contributions from:

Dr. Rosa García

Jacobs University Bremen

Dr. Eric Epping

Royal Netherlands Institute for Sea Research

Master Thesis

August 2010

Contents

Acknowledgements	3
Abstract	4
1. Introduction	5
2. Study Area	6
2.1 Geographical and Geomorphologic setting	6
2.2 Oceanographic and Atmospheric settings	6
2.3 Particulate matter input, transport and deposition	8
3. Materials and methods	10
3.1 Sediment collection	10
3.2 Geochemical and sedimentological analyses	10
3.3. Benthic foraminifera	12
3.3.1 <i>Recovery of benthic foraminifera from sediment samples</i>	12
3.3.2 <i>Foraminiferal data analysis</i>	13
4. Results	15
4.1 Environmental setting: Geochemical parameters	15
4.1.1 <i>Food quality and quantity: sedimentary phytopigments, organic carbon and total nitrogen</i>	15
4.1.2 <i>Sedimentary redox conditions: pore water nitrate and ammonium</i>	17
4.1.3 <i>Sediment grain size</i>	17
4.2 Surface and in-sediment benthic foraminifera distribution	21
4.2.1 <i>Total Standing Stocks, Diversity and the Average Living Depths of foraminifera</i>	21
4.2.2 <i>Down-core species distribution, group abundances and species assemblages</i>	24
4.2.3 <i>The arborescent and tubular agglutinated foraminifera</i>	28
4.2.4 <i>The core top 63-150 µm fraction benthic foraminifera</i>	29
4.3. Environmental parameters and benthic foraminifera distribution: the TROX (Trophic-Oxygen) model	32
4.4 Environmental control on the spatial distribution of benthic foraminifera	35
5. Discussion	37
5.1 Canyon versus open slope: benthic environments as a function of food quantity and quality	37
5.2 The dynamics between food supply, physical disturbance and benthic foraminiferal community structure ..	39
5.3 Benthic foraminiferal assemblages from different trophic regimes	40
5.3.1 <i>Benthic foraminifera from eutrophic environments</i>	40
5.3.1 <i>Benthic foraminifera from mesotrophic environments</i>	41
5.3.1 <i>Benthic foraminifera from oligotrophic environments</i>	42
5.4 Arborescent and tubular agglutinated foraminifera in the Cap de Creus canyon and slope areas	43
5.5 Cap de Creus canyon benthic foraminifera in comparison to other canyon systems	44
6. Conclusions	47
7. References	48
8. Appendix	52

Acknowledgements

The completion of this report was only possible thanks to the support and help of my supervisors, family and friends who motivated me until the end of the writing process.

I would like to thank my main supervisor Karoliina Koho for all the varied things that I learned working with her. In principle, for the new insight she gave me into the world of foraminifera; but mainly, because through the entire development of this research I always felt part of a team. I thank her for all the dedicated hours that she spent guiding me, from the taxonomic identification to the detailed revision and correction of this manuscript, and for her opportune comments, suggestions, ideas and answers to my varied questions.

Especial thanks are dedicated to Henko de Stigter for his kind help in several crucial moments of this research. In first place, for coordinating the collection of the analyzed material. In second place, for shearing the sedimentological data incorporated in this study. In third place, for helping me with the data analysis and for assisting to the presentation of results. But especially, for dedicating invaluable time in reading and commenting the final manuscript. His opportune observations improved considerably the quality of this work.

I would like to thank Ivo Duijnste for his help and advice with the statistical analysis of the data. In particular for making time in his extremely busy schedule to have a careful look to the data and for performing miracles with several different computers to make the analysis possible. The results that came out from it were very important in the interpretation of the data.

Also many thanks to Lucas Lourens for the time he dedicated to the reading of this manuscript.

Many thanks as well to Geert Ittman for helping me with the washing of the samples and for giving me a friendly welcome into the lab. His kind help made me easier to keep up with my tight schedule.

Also special thanks are dedicated to Tanja Kouwenhoven for assisting to the presentation of results, for sharing her knowledge on the taxonomic identification of doubtful species and especially for her enthusiasm and help in my participation on the Darwin Days 2010.

Especial thanks to Rosa García, Eric Epping and Erica Koning for their kind contribution sharing the geochemical data that made possible the elaboration of this study.

To Andy Gooday for sharing with us his invaluable expertise in the taxonomic determination of strange species of forams.

Many thanks to Ingrid Beekman for being so kind to me during all the administration procedures. Her opportune advice and help were crucial for the completion of my masters on its due time.

To the members of the Stratigraphy and Paleontology group, for their direct and indirect contributions to the realization of this research.

To all my friends in Utrecht who gave color to my time here, especially to Anne, Aileen, Ciara, Adriana and Frederike.

To Jasper, for his love, his patience and support in the most difficult moments of my time here in the Netherlands and for believing in me so strongly. To his family, Robin, Robert y Annemarie, for giving me such a warm welcome into the Netherlands and into their lives.

A todos mis amigos en México, por su invaluable amistad, por creer en mí y apoyarme en mis locos proyectos. En especial, Karla, Ceci, Fred, Adrián, Bárbara y Adrianita. Por compartir conmigo mis aventuras y desventuras con tanto cariño.

A mi querida familia en México, Diana, Mamá, Papá, tías Beatriz y Mónica, tío Valentín, Mariana y Rebeca, y mis queridos abuelitos. En estos dos años los he llevado en mi corazón y en mis pensamientos todos los días con la mayor añoranza y cariño. Su inestimable apoyo me ha impulsado más lejos de lo que jamás pensé. Siempre les estaré agradecida a todos y cada uno de ustedes. Abuelitos... siempre están y estarán conmigo.

Abstract

Currently, the Cap de Creus canyon experiences dense water cascading (DSWC) events with seasonal frequency and decadal peaks in intensity. These events transport suspended organic particles which could potentially sustain higher biological productivity inside the canyon in comparison to the adjacent slope. To investigate this, Rose Bengal stained samples were collected along a depth transect over the Cap de Creus Canyon and its adjacent slope. Benthic foraminifera were studied in the top 5 cm of sediment, and faunal abundances and assemblages were compared against geochemical data. Results indicate that the decrease of food quality (Chl *a*/Phaeo ratio), with increasing water depth, is the main factor determining the distribution of foraminifera species both in canyon and slope environments. The decrease of food quantity (CPE concentration), which appears to be somewhat higher in the canyon than open slope environments at equivalent water depths, represents the second most important factor. However, as the contrast with the slope is largest in the canyon head and the upper canyon, the DSWC seem to influence mostly these settings. Thus, eutrophic conditions were only found at the canyon head, dominated by the species *Ammoscalaria pseudospiralis*, *Cibicides ungerianus*, *Cassidulina laevigata*, and *Bolivina spathulata*. Mesotrophic environments occurred in the shallow open slope and around the middle canyon section. Assemblages were dominated by *Uvigerina mediterranea*, *Bigenerina nodosaria*, *Bolivina spathulata* and *Eponides pusillus*. *Chrithionina cf. mamilla* was abundant inside the canyon probably profiting from currents activity. The canyon sites at these water depths were also abundant in arborescent and tubular foraminiferal fragments, (especially *Saccorhiza ramosa* and *Dendrophrya* sp.). Oligotrophic environments occurred in the deepest canyon and slope areas and were dominated by *Ammolagena clavata*, *Glomospira charoides* and an unidentified single-chambered “agglutinated dome” species. *E. pusillus* was also abundant in these environments probably profiting from the hemipelagic rain of particles from the early spring phytoplankton bloom. Our results are in good agreement with previous studies of foraminifera from submarine canyons and deep-sea environments; however, our data highlight that submarine canyons are complex systems, each modified by a number of local processes that are specific for the setting.

1. Introduction

Benthic foraminifera have long been used as ecological proxies for marine environments because they are a successful group that can survive and proliferate under a wide range of environmental conditions (Jorissen et al., 2007). Their ecological role becomes particularly important in deep-sea environments, where they can constitute up to 50% of the total biomass (Gooday et al., 1992). It is currently accepted that the distribution of benthic foraminifera in marine sediments is principally driven by the availability of organic matter as food source (Jorissen et al., 2007). In particular, the seasonal deposition of phytodetritus, the labile fraction of organic matter, has been considered crucial for the proliferation of benthic foraminiferal faunas in deep-sea environments (Gooday, 1988; Gooday and Hughes, 2002). Benthic foraminifera are generally found in the top 5 to 10 cm of sediment. Their in-sediment distribution, or microhabitat, has been described by the TROphic Oxygen (TROX) model of Jorissen et al. (1995). This model proposes that in oligotrophic well-oxygenated environments the vertical distribution of benthic foraminifera is limited to the surface sediments by low food supply, whereas in eutrophic poorly-oxygenated environments, the vertical distribution is restricted by the steep redox gradients. Therefore, it is in meso-eutrophic environments where the highest standing stocks and diversity tend to occur and communities extend deepest into the sediments (Jorissen et al., 1995). Since the distribution, abundance and diversity of benthic foraminifera is so closely linked to the availability of labile organic matter, it is to be expected that environments rich in labile organic matter will display high abundances and diversity of benthic foraminifera. Submarine canyons could be an example of such environments due to their important role in sediment and organic matter transport from the continental shelf into the abyssal plains (Canals et al., 2006). Furthermore, higher organic carbon concentrations have been reported to occur inside submarine canyons in comparison to adjacent slope environments (de Stigter et al., 2007; García et al., 2008; Koho et al., 2008; Koho et al., 2007; Schmiedl et al., 2000).

A few previous studies on living foraminiferal communities in submarine canyons have shown that canyons can sustain higher and more diverse benthic foraminiferal faunas than their adjacent environments (Fontanier et al., 2008; Koho et al., 2008; Schmiedl et al., 2000). The development of these communities, however, depends ultimately on the balance between food supply, sediment erosion and physical disturbance. Where the last two are higher than the first one, benthic foraminiferal communities cannot prosper (Koho et al., 2007). On the other hand, high organic matter concentration in the sediments, and the increased oxygen consumption associated to its degradation, induce steeper redox gradients that may be limiting for many species (Koho et al., 2008). To further our understating of these unique environments and the ecosystems that they support, living benthic foraminifera were sampled from the Cap de Creus canyon on the western Mediterranean. This canyon exposes particular characteristics, experiencing dense shelf water cascading (DSWC) with seasonal frequency and with decadal peaks in intensity. These powerful events transport organic matter, including partially degraded and fresh marine and

terrestrial organic matter, from the outer continental shelf towards the canyon (Sánchez-Vidal et al., 2009). Even more, DSWC season overlaps with the phytoplankton spring bloom (Fabres et al., 2008), which may further increase the potential amount of labile organic matter transported into the canyon. Thus the aims of this study are (1) to investigate the influence of the geochemical parameters on the abundance and distribution of benthic foraminifera in the Cap de Creus canyon and adjacent open slope area, and (2) to determine if canyon environments can sustain more abundant and more diverse benthic foraminifera standing stocks than adjacent open slope environments. Since samples were collected at the end of the cascading season, the canyon is expected to be a more eutrophic environment than the adjacent slope and capable of sustaining higher biological productivity.

2. Study Area

2.1 Geographical and Geomorphologic setting

The Cap de Creus Canyon is located at the southwestern end of the Gulf of Lions in the northwestern Mediterranean (Fig. 1). The Gulf of Lions is a microtidal margin dominated by river discharge and waves (Palanques et al., 2006). The continental shelf is a passive tectonic margin with crescent shape that displays a maximum width of 72 km, narrowing towards the west to less than 15 km near Cap de Creus (de Geest et al., 2008). The shelf break is incised by an intricate network of at least 10 submarine canyons that extend through the continental slope coalescing into two primary channels on the deep slope down to a complex continental rise (de Geest et al., 2008; Lastras et al., 2007). The Cap de Creus Canyon has an axial length of 96.1 km across the continental slope and rise. The axis presents a general west-east direction and at the deepest end it joins to the Sète Canyon. On the basis of mean slope, gradient, orientation, width and other morphologic criteria, four sections can be recognized: canyon head, upper canyon, middle canyon and lower canyon (Table 1; after Lastras et al., 2007).

2.2 Oceanographic and Atmospheric settings

The oceanic circulation in the Gulf of Lions is dominated by the Liguro-Provençal-Catalan current, also known as the Northern current, which creates a net east-to-west cyclonic circulation along the outer shelf (de Geest et al., 2008). The Northern current is constrained by the coast inshore and by a thermo-haline along-slope current offshore (Canals et al., 2006). The result is that most of the water of the Northern current funnels towards the Cap de Creus promontory along the narrowing southwestern shelf and is, thus, deviated towards the Cap de Creus Canyon.

The atmospheric circulation is dominated by two main wind systems: continental and marine (Palanques et al., 2006; Ulses et al., 2008). Continental winds, known as Tramontane (northwestern) and Mistral (northern), have a cold-dry nature and predominate during winter. In contrast, marine winds, blow from south-southeast directions, are episodic and short-lived. They are associated with marine storms and usually occur episodically from autumn to spring (Ulses et al., 2008). The blow of the continental winds over the sea during winter causes intense cooling of the surface water. This cooling produces an important increase of water density and the disappearance of the thermocline, which facilitates dense water formation (Palanques et al., 2006). The dense water sinks in order to reach its level of neutral buoyancy, and may reach the shelf break and cascade through the numerous canyons that intersect the continental slope of the Gulf of Lions (Canals et al., 2006; Palanques et al., 2006). The equilibrium depths for the dense water masses range from 170 to 800 m; however, in extraordinary cold winters (e.g. 1998-99 and 2004-05) cascading waters reached depths beyond 1000 m (Canals et al., 2006).

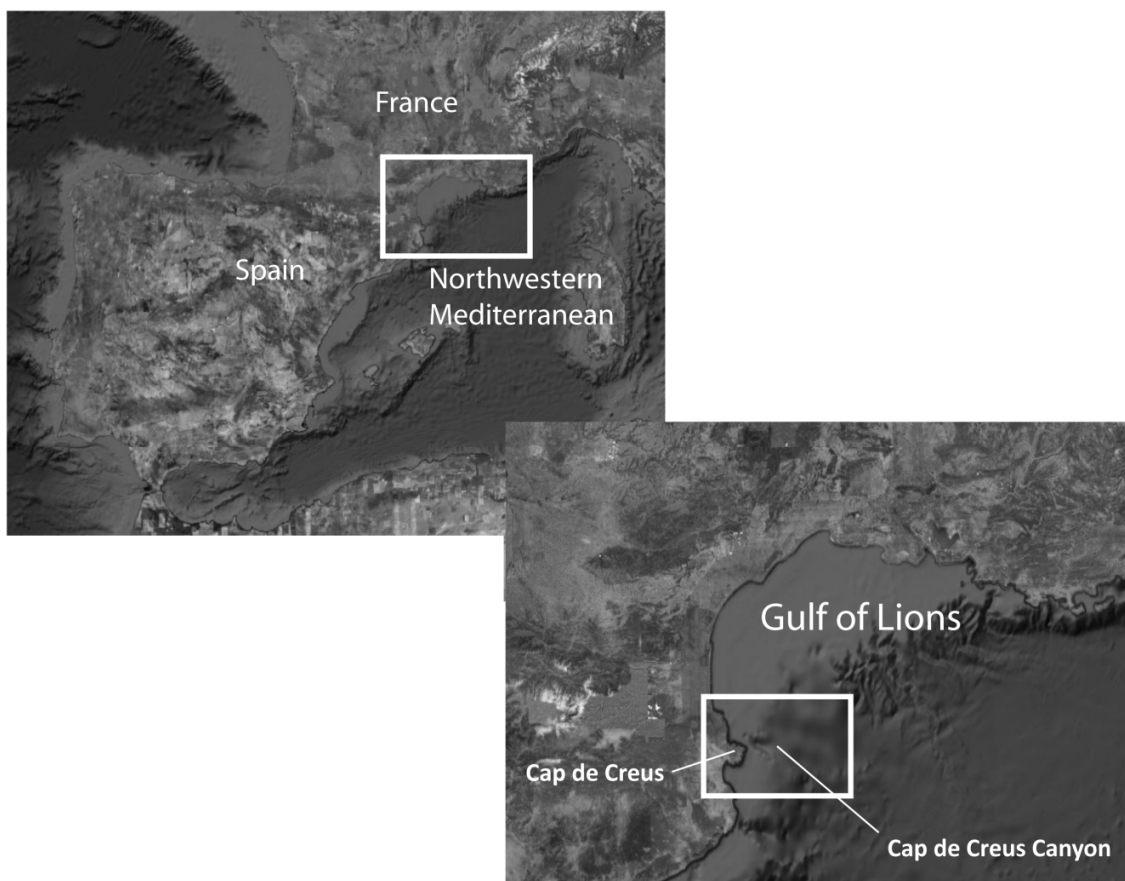


Fig. 1. Location of the Gulf of Lions and the Cap de Creus Canyon in the Northwestern Mediterranean. Images modified from Google Earth 2010.

Dense water cascading (DWC) can have particular high intensity in the Cap de Creus canyon (in comparison with other canyons of the area), given the funneling of surface currents at the southwestern end of the Gulf of Lions. Cascading occurs mainly over the southern flank of the canyon, as a result of the cyclonic nature of the ocean circulation. During strong marine storm events, downwelling of surface water can be induced as a result of massive convergence of water at the southwestern end of the Gulf of Lions (which results from intensified currents and increased precipitation and river discharge during the storm) (Ulses et al., 2008). Water downwells into the nearby canyons heads (down to 300-400 m); however, the stratification of the water column can restrict the intrusion of the downwelling water avoiding it to reach greater depths (Ulses et al., 2008).

2.3 Particulate matter input, transport and deposition

The main sources of particulate matter to the shelf waters in the Gulf of Lions are: riverine discharge, atmospheric dust transport (primarily Saharan dust), marine biological production and particle resuspension during storms and cascading events (Heussener et al., 2006).

The Rhône river is the main supplier of freshwater and sediment of the Gulf of Lions. With an average discharge over $1000 \text{ m}^3 \text{ s}^{-1}$ (Bourrin et al., 2008), it delivers more than 80% of the total freshwater input (Sánchez-Vidal et al., 2009) and more than 90% of the total sediment input (Tesi et al., 2010). The Rhône discharges an annual organic carbon input of $19.2 \pm 6 \cdot 10^4 \text{ t C year}^{-1}$, whereas the total river input for the Gulf of Lions is estimated in $24 \pm 10 \cdot 10^4 \text{ t C year}^{-1}$ (Tesi et al., 2007). In addition, three small rivers (the Agly, the Têt and the Tech) discharge in the slope nearby the Cap de Creus Canyon head, with an average discharge of less than $10 \text{ m}^3 \text{ s}^{-1}$ (Palanques et al., 2008). The finest sediment fraction of the river discharge remains in suspension near the sea floor forming a thick turbid layer known as benthic nepheloid layer (BNL) that also follows the trajectory of the Northern current (Tesi et al., 2010). The BNL becomes thinner offshore, but thickens at the canyon heads where it develops up to intermediate depths, becoming an important sediment export vector from the shelf to the slope (Tesi et al., 2007). The river supply becomes maximum during marine storms since these ones are often accompanied by river floods that result from excess of precipitation (Ulses et al., 2008).

During marine storm events most of the resuspended sediments are usually deposited again within the shelf, but part of it can reach the canyon heads by the downwelling of surface water associated to the storm (Fabres et al., 2008). However, the only way in which sediments can be effectively funneled down-canyon is if they are carried by dense water cascades. Cascading water erodes the canyon head and upper canyon sections and redeposits the sediments down canyon (de Geest et al., 2008). The BNL particulate matter input dominates down slope fluxes during pre- and post cascading periods (Tesi et al., 2010).

Table 1. Cap de Creus Canyon subdivision and main characteristics. Subdivision after Lastras et al. (2007).

	Canyon head	Upper canyon	Middle Canyon	Lower canyon
Cross-section shape	V	V	V	U
Depth range	125-400 m	400 – 1000 m	1000-1600 m	1600-2100 m
Morphology	Thalweg: constant width of ~600 m Southern flank: irregular Northern flank: regular (1)	Thalweg: widening up to 6.5 km Rounded gullies on the top of the northern flank (1)	Southern flank is 700 m height, the top of the wall constitutes the shelf break Northern flank is 500m wall height (1)	Southern flank is >100 m high (1) Destabilization of the lower part of the northern flank (~1800m) narrows the thalweg (1)
Physical disturbance	DWC and surface water downwelling, both phenomena with seasonal periodicity (2, 6)	DWC affecting mostly the southern flank and the lowest part of the northern flank (1) Cascading can have seasonal occurrence with interannual intensity variations (7)	DW cascading under extraordinary cold conditions, mostly decadal frequency (3, 7)	
Bedforms		Mega-scale furrow field hanging 50 m above the thalweg in all the southern flank and the lowest part of the northern flank (1, 5)	Mega scale furrows along the southern flank, mega furrows along the low northern flank (1)	Faults on the sea floor rooted in Mesinian evaporates, mega-scale ponds and ripples (1)
Depositional environment	Erosional (4)	Southern flank erosional, Northern flank mostly depositional (4)	Southern flank erosional, Northern flank mostly depositional (4)	Thalweg erosional (1)
Sedimentology	Coarse grained material up to ~400 m depth (4) Presence of coarse shell fragments (6)	Mud layer present in the thalweg around 400-780 m that is periodically flushed, silty clays in the northern flank, sand and gravels in the southern flank (4)		
Sedimentation rate		5-10 mm yr ⁻¹ for the thalweg mud layer, Northern flank has average accumulation rates of >1.5 mm yr ⁻¹ , Southern flank sedimentation rates range from 0 to 0.5 mm yr ⁻¹ (4)		
Particulate matter fluxes	During DWC, SSC* are bigger than 68 mg L ⁻¹ , SSF** surpass 52.07 g m ⁻² s ⁻¹ (2), while total organic carbon fluxes are ~50 g C m ⁻² yr ⁻¹ (3) During marine storms, SSC get to 48 mg L ⁻¹ , while SSF get to 31.12 g m ⁻² s ⁻¹ (2)			

References: (1) Lastras et al. (2007), (2) Palanques et al. (2006), (3) Canals et al. (2006), (4) DeGeest et al. (2008), (5) Puig et al. (2008), (6) Ulises et al. (2008), (7) Herrman et al. (2008).

* Suspended sediment concentration

** Suspended sediment flux

3. Materials and methods

3.1 Sediment collection

The sediment samples for this study were collected on board of the RV “Pelagia” of Royal NIOZ during the cruise 64PE225 in May 2004, as part of the EUROSTRATAFORM project. Multicore samples were collected with a MUC 8+4 multiple corer developed by Oktopus GmbH, constituted by eight 6 cm and four 10 cm diameter coring tubes of 61 cm length. Seven stations were studied in total, four from the Cap de Creus canyon and three from the adjacent slope (Table 2 and Fig. 2).

Table 2. Sampled stations at the Cap de Creus canyon and adjacent slope during the cruise 64PE225. The location of stations inside the canyon or on the adjacent open slope is indicated as well as their geographic coordinates. The water depth and the distance to Cap de Creus are also specified.

Station	Location	Latitude (N)	Longitude (E)	Water depth (m)	Distance to land* (km)
52	canyon	42° 23.27'	03° 19.80'	344	7.0
54	slope	42° 14.00'	03° 35.48'	343	24.1
50	canyon	42° 15.97'	03° 40.05'	1215	28.8
51	slope	42° 18.01'	03° 54.00'	1209	47.3
47	canyon	42° 10.40'	04° 04.19'	1801	63.4
49	slope	42° 07.49'	04° 03.45'	1874	64.1
48	canyon	42° 14.95'	04° 20.76'	2112	84.2

* Cap de Creus used as the nearest land point for all the stations

3.2 Geochemical and sedimentological analyses

Sediment pore water was analyzed to obtain down core profiles of dissolved nitrate (NO_3^-) and ammonium (NH_4^+). The cores were sliced on board immediately after their recovery with a hydraulic slicer at *in situ* temperature. The top cm of sediment was sliced every 0.25 cm, between 1 to 3 cm slices were taken every 0.5 cm, between 3 and 7 cm slices were taken every 1.0 cm and below 7 cm the slicing was performed every 2 cm. The sediment samples were centrifuged at 3000 rpm for 10 minutes. The recovered supernatant was then filtered using 0.45 μm Acrodisc filters, and analyzed on board for nitrate, following the methods described by Grashoff et al., (1983), and ammonia, according to the method described by Helder, (1989), on a TRAACS-800+ autoanalyser. The remaining sediment

pellets were frozen at -20° and stored for solid phase (C and N) analyses. Sedimentary carbon, total nitrogen and organic carbon were measured with a Thermo Finnigan flash element analyzer following the procedures described by Lohse et al. (2000). The analytical precision of the carbon and nitrogen analyses was always within 0.3–1.5%. The CaCO_3 was calculated as the difference between total carbon and organic carbon.

Nitrate penetration depth (NPD) has been used as an indicator for the redox conditions within the sediment column as nitrate is produced during nitrification, a process that consumes oxygen (Jensen et al., 1994) and requires its availability to take place. Since ammonium is the prime matter for nitrification, it can only start accumulating in the sediments when no more nitrification is taking place. In addition, nitrate is the second most favorable electron acceptor after oxygen and, therefore, it starts being removed from the sediments once oxygen is depleted. Nitrate (NO_3^-) and ammonium (NH_4^+) curves were used to calculate the nitrate penetration depth (NPD), estimated to be the depth in the sediment where nitrate is depleted and ammonium starts building up.

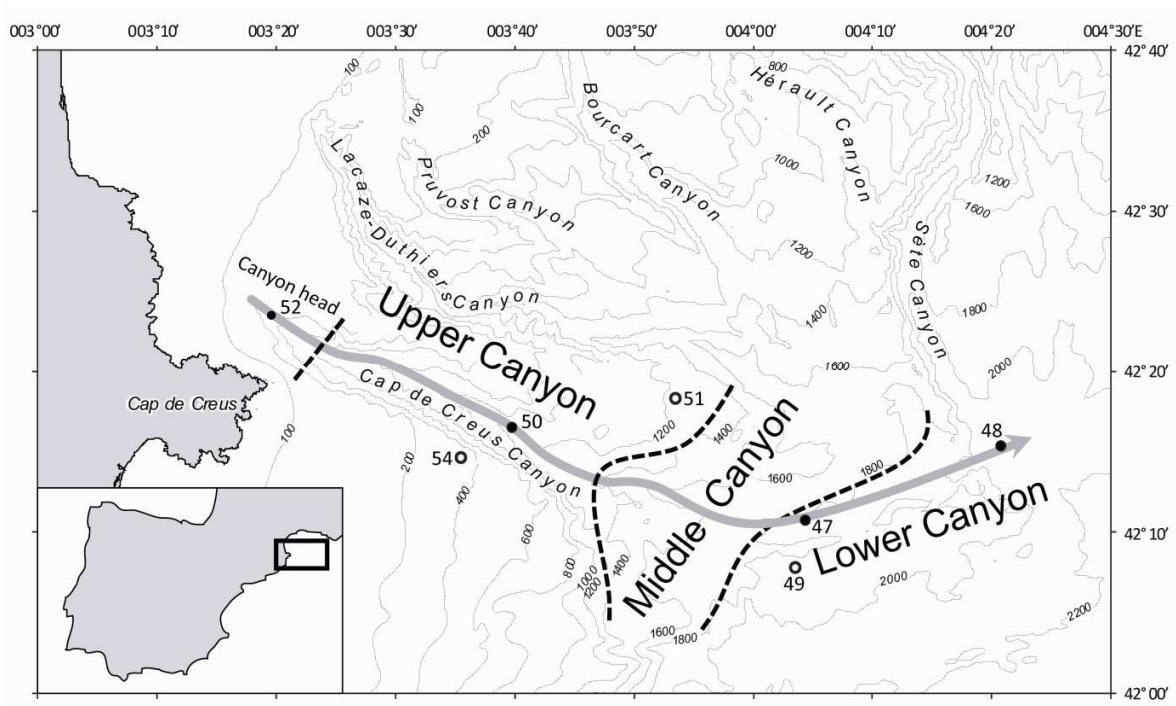


Fig. 2. Map of the Cap de Creus Canyon with the seven sampled stations: canyon stations in closed circles, slope stations in open circles. Canyon subdivision into upper, middle and lower sections after Lastras et al. (2007).

For the analysis of phytopigments (Chlorophyll-*a* and phaeopigments), the cores were sliced at 0.5 cm intervals down to 1 cm, at 1 cm intervals from 1 to 5 cm, at 2 cm intervals from 5 to 9 cm and at 3 cm intervals from 9 to 15 cm. The methods for the determination of phytopigment concentrations are described by García et al.(2008). The

phytopigments (chlorophyll-a + phaeopigments) content in the sediment is termed “chloroplastic pigment equivalents” (CPE) after Thiel et al. (1978). CPE comprehends both fresh (Chlorophyll *a*) and semi-degraded pigments (phaeopigments) in order to estimate the total amount of potential food available for benthic foraminifera. The freshness of this food is further estimated by the chl *a*/phaeo ratio, with a higher ratio indicating higher food quality. On the other hand, organic carbon (C_{org}) has been used as an alternative indicator for food abundance, while the C_{org}/N ratio has been used as an alternative indicator for food quality. The latter is also an indicator of the terrestrial or marine origin of the organic matter and thus, also of its degradability. Marine organic matter is considered fresher because it is produced “in situ” while terrestrial organic matter has to be transported and, in the mean time, is submitted to different degrees of degradation. Besides, terrestrial organic matter is usually composed of complex molecules, like lignin and cellulose, which makes it more refractory to degradation. Terrestrial plants tend to be richer in carbon (C/N 20-500) in comparison to plankton (C/N \approx 7) (Hedges et al., 1997) and, in consequence, C/N ratio values higher than 15 are considered to indicate organic matter of terrestrial origin.

The sediment grain size was determined using a Coulter LS230 laser particle sizer; the full description of the methods can be found in de Stigter et al. (2007).

3.3. Benthic foraminifera

3.3.1 Recovery of benthic foraminifera from sediment samples

For analysis of benthic foraminifera, cores were sliced every 0.5 cm down to 2 cm, and every 1 cm down to 10 cm. Immediately after slicing, the samples were treated with a solution of Rose Bengal in 96% ethanol (1 g/L) and stored in sealed plastic bags until further treatment.

In the laboratory, the sediment samples were wet-sieved into the >150 and $>63-150$ μm fractions. After sieving the samples were oven dried at 60 °C and stored in glass containers. For each station, the >150 μm fraction of the top 5 cm of sediment were analyzed. The Rose Bengal stained foraminifera were wet picked from a Petri dish, containing 50% ethanol, under a stereoscopic microscope. In all cases, only the well-stained specimens were considered as living, while patchy coloration was considered an indicator of dead-specimens at the time of sampling. If the presence of stained protoplasm was unclear, the test was broken with the aid of a needle and the protoplasm further inspected. The stained foraminifera were placed in micropaleontological plates; counted and identified to the highest taxonomic level possible. In case of station 52, which contained abundant, large shells fragments, sediment was additionally dry-sieved over 1 mm mesh. This fraction was separately checked for encrusting, or very

large, Rose Bengal stained foraminifera. Furthermore, splits of surficial sediment (0-0.5 cm) of the 63-150 μm fraction were briefly examined for benthic foraminifera; the aim of this exercise was merely to get a picture of the most abundant species in the small size class. The estimation of TSS per station of this fraction is sometimes based on relatively few specimens and thus should be considered with caution.

Benthic foraminifera were subdivided, when relevant, within four groups for analytical purposes: calcareous perforate (denoted here as Hyaline), calcareous imperforate (denoted here as Porcelaneous), multilocular and single-chambered agglutinated (denoted here just as agglutinated) and arborescent and tubular agglutinated (denoted here just as arborescent and tubular). This division has been made to facilitate the comparison with other studies and is based on the differences in the ecological response of the four different groups in relation to food quality and quantity. This division also facilitates comparison of the results with paleoceanographic studies since most agglutinated species are too fragile to be preserved in the geological record.

Arborescent and tubular agglutinated foraminifera break easily, and thus it is difficult to distinguish single individuals. In this study the fragments were considered as complete individuals if a middle bulge or terminal bulb was present and the protoplasm was evenly spread along the tube. In any other case, well stained specimens were counted as fragments (see Koho et al. 2007, 2008 for comparison).

3.3.2 Foraminiferal data analysis

The total standing stocks (TSS) of foraminifera per core were calculated by adding up the number of stained specimens found in top 5 cm of sediment. TSS per core thus represents the number of living foraminifera under an area of 28.3 cm^2 . In order to facilitate the comparison between the different depth intervals, the individual counts of each sediment sample were standardized to a volume of 50 cc (cubic centimeters). Therefore, all the results are reported here in densities per 50 cc. Relative abundances per benthic foraminifera group (hyaline, porcelaneous, agglutinated, arborescent and tubular agglutinated) and per species were determined for core-slices and for complete cores.

Diversity was evaluated by determining the species richness (S), which is the total number of species, and by the Shannon index (H' ; Murray, 2006) according to the formula:

$$H' = -\sum_{i=1}^S (p_i \ln p_i) - [(S-1)/2N]$$

Where p_i is the relative abundance of each species, calculated as the proportion of individuals of a given species to the total number of individuals in the community (n_i/N), n_i is the number of individuals in species i , S is the species richness, and N is the total number of all individuals. However, for any given number of species there is a maximum possible H' , denoted as H_{\max} , which occurs when all the species are present in equal numbers, and is calculated as follows:

$$H_{\max} = -\sum_{i=1}^S \frac{1}{S} \ln \frac{1}{S} = \ln S$$

The quotient between H' and H_{\max} is a measure of the evenness (E) of the diversity within the community,

$$E = \frac{H'}{H_{\max}}$$

Average living depth (ALD), after Jorissen et al. (1995), was used as an indication of the vertical distribution of the TSS and of individual species. ALD were determined only for species with at least three specimens per sample, and were calculated as follows:

$$ALD = \sum_{i=0,x} (n_i D_i) / N$$

Where x corresponds to the lower boundary of the deepest sample, n_i represents the number of benthic foraminifera in the interval i , D_i is the mid-depth of the sample interval i , and N is the total standing stock for all sediment depth levels.

Pearson correlation analysis was performed, with the software SPSS for Windows, to evaluate the relationship between TSS and different environmental parameters. Additionally, a Detrended Correspondence Analysis (DCA) was carried out, with the software CANOCO for Windows, to further investigate these relationships and the different responses between the foraminiferal communities in the canyon and in the slope. The analysis was detrended using the method of the second order polynomial. Species were selected from both the 63-150 μm and the >150 μm fractions. Rare species (>1% RA) were left out as well as geochemical parameters with incomplete data sets.

4. Results

4.1 Environmental setting: Geochemical parameters

4.1.1. Food quality and quantity: sedimentary phytopigments, organic carbon and total nitrogen

Chloroplastic pigment equivalents (CPE) concentrations showed a general decrease trend with increasing water depth (Fig. 3A); however, this trend was not statistically significant since the concentrations at the shallowest slope station (54-S) showed a large offset. Furthermore, canyon stations always displayed higher CPE concentrations than open slope stations at comparable water depth. Thus, the highest surficial CPE concentration occurred in the canyon head, at station 52-C ($14.54 \mu\text{g cm}^{-3}$) followed by stations 54-S and 50-C (3.20 and $3.33 \mu\text{g cm}^{-3}$), respectively. The difference in surface CPE concentration between the shallowest and the deepest station inside the canyon was of almost one order of magnitude ($14.54 \mu\text{g cm}^{-3}$ at station 52-C and $2.18 \mu\text{g cm}^{-3}$ at station 48-C), whereas it was almost five times between the canyon head and the open slope at comparable water depth ($3.20 \mu\text{g cm}^{-3}$ at station 54-S). Almost in all cases, the CPE concentrations decreased down-core (Fig. 4). The decline is sharp and already at 1.5 cm depth in sediment the concentrations were between two to six times lower than at surface (e.g. $14.54 \mu\text{g cm}^{-3}$ at 0.25 cm and $7.17 \mu\text{g cm}^{-3}$ at 1.5 cm in station 52-C; $3.04 \mu\text{g cm}^{-3}$ at 0.25 cm and $0.48 \mu\text{g cm}^{-3}$ at 1.5 cm in station 51-S; $2.18 \mu\text{g cm}^{-3}$ at 0.25 cm and $0.41 \mu\text{g cm}^{-3}$ at 1.5 cm in station 48-C; Fig. 4). The contrast between the surface and deep sediment CPE concentrations tended to decrease when going from shallower to deeper stations (Fig. 4). CPE concentrations presented a highly significant positive correlation with Chl *a* ratios and with ammonium concentrations (Table 3).

The surficial Chl *a*/Phaeo ratio was higher for shallow stations (0.05 at stations 52-C and 54-S), however it did not show a strong decrease towards deeper stations (0.03 at stations 50-C, 51-S, 49-S and 48-C; 0.02 for station 47-C) (Fig. 3A). The difference between canyon and open slope was minimum at shallow stations (52-C and 54-S) but increased towards deeper stations where it was the ratio was higher on the slope at comparable water depths. The Chl *a*/Phaeo ratio tended to decrease down-core in most of the stations (Fig. 4). The only exception was station 47-C, which showed a maximum ratio between 1.5 and 2.5 cm (0.23 - 0.27). The difference between surface and the deepest (4.5 cm) in-sediment ratio values was of 0.02 for stations 52-C and 54-S, and 0.01 for all the other stations. Chl *a*/Phaeo ratios showed a significant positive correlation with median grain size and a significant negative correlation with water depth (Table 3).

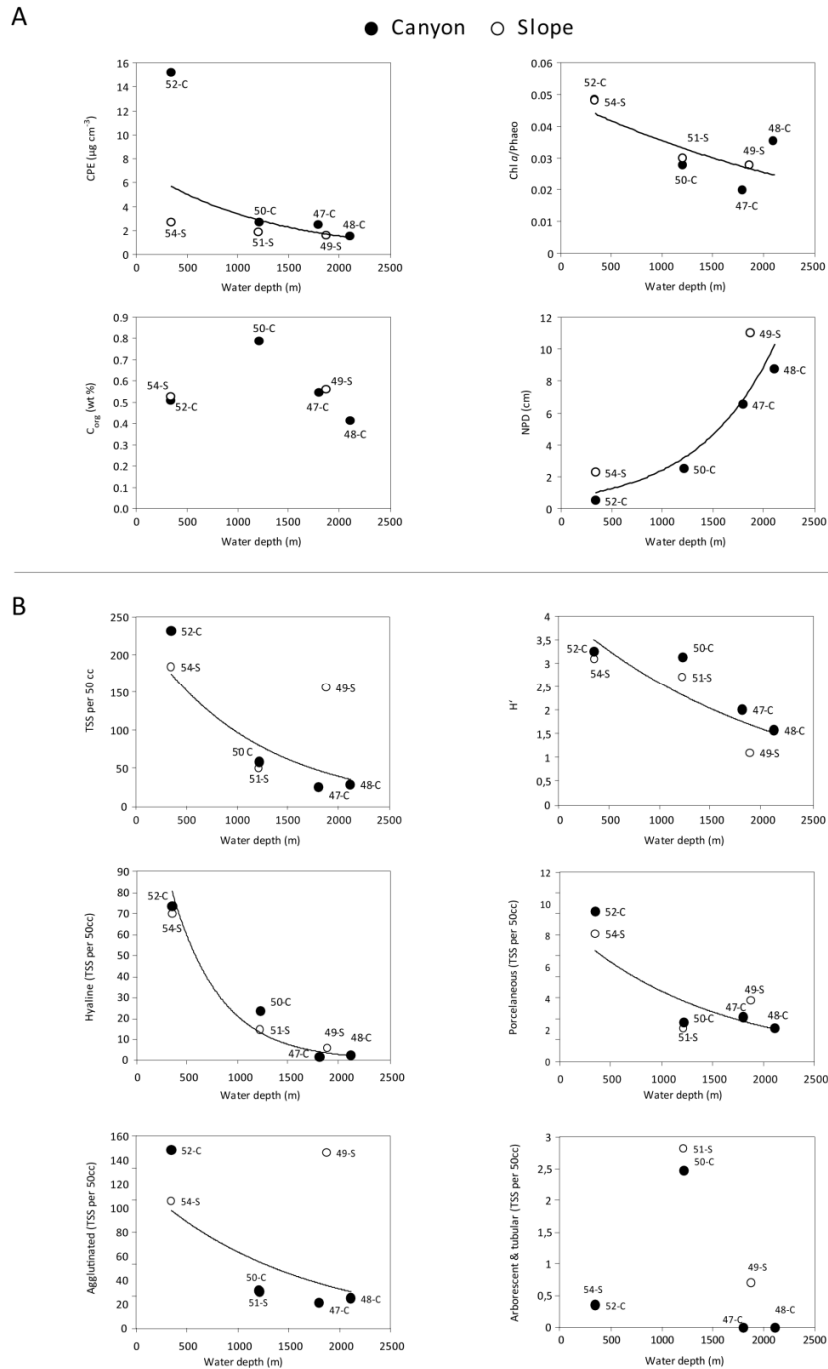


Fig. 3. Trends of (A) benthic foraminifera TSS and diversity, and (B) selected environmental parameters in function of water depth. All TSS are standardized for 50 cc. Trend lines are indicated when there is a trend. All stations are plotted together; however, canyon stations are presented with closed circles whereas slope stations are presented with open circles. (A-i) Total standing stock for all benthic foraminifera per station, (A-ii) Shannon diversity index (H'), (A-iii) hyaline benthic foraminifera TSS, (A-iv) porcelaneous benthic foraminifera TSS, (A-v) agglutinated benthic foraminifera TSS, (A-vi) arborescent and tubular benthic foraminifera TSS. (B-i) Chloroplatic pigments equivalents (CPE), (B-ii) chlorophyll-a:phaeopigments ratio, (B-iii) bulk organic carbon, (B-iv) nitrate penetration depth (NPD).

Sedimentary organic carbon (C_{org}) values did not show a clear trend either with water depth or any other parameter in the canyon and slope environments (Fig. 3A, Table 3). The overall surface and in-sediment C_{org} concentrations varied between 0.3 and 0.7% but did not change consistently with water or sediment depth. Similarly, no trend was seen in the C_{org}/N ratio; values ranging between 4 and 10. The highest C_{org}/N ratio of 11.6 was found at the surface of the shallow station 52-C followed by station 47-C with a surface C_{org}/N ratio of 11.3. The lowest value (ratio of 3.7) was recorded at the surface sediments of the deepest canyon station 48-C.

4.1.2 Sedimentary redox conditions: pore water nitrate and ammonium

Nitrate concentrations ranged from $2.5 \mu\text{mol L}^{-1}$ at 1 cm sediment depth in station 52-C up to $16.7 \mu\text{mol L}^{-1}$ at 2.5 cm sediment depth in station 49-S (Fig. 4). Ammonium concentration ranged from $0.5 \mu\text{mol L}^{-1}$ at the core top of station 54-S up to $36 \mu\text{mol L}^{-1}$ at 4.5 cm sediment depth in station 52-C (Fig. 4). Ammonium concentrations displayed a highly significant positive correlation with CPE and Chl a concentrations, whereas nitrate concentrations had a significant negative correlation with C_{org}/N ratios (Table 4).

The nitrate penetration depth (NDP) was minimum in the shallow stations and maximum at the deep stations (Table 4, Fig. 3). The shallowest NDP occurred at the canyon head in station 52-C (0.5 cm), whereas the deepest NDP was recorded at deepest slope station 49-S (11 cm). NDP was always shallower in canyon station than in slope stations at similar depth (Fig. 3). For example, NDP at station 54-S, at 343 m WD, was almost the same that at station 50-C, at 1215 m WD, with values of 2.25 versus 2.5 cm respectively. Whereas the deepest station 48-C, at 2112 m WD had a shallower NDP (8.75 cm) than station 49-S at 1874 m WD. NDP showed a significant positive correlation with water depth and distance to the shore (Table 3).

4.1.3 Sediment grain size

Sediments in all the stations were predominantly composed by silt particles (vol. %), although its proportion increased inside the canyon and towards shallower areas. However, the in-sediment grain-size distribution was especially variable inside the canyon, which highlights the heterogeneity of the system. Stations 52-C (344 m WD) and 50-C (1215 m WD) were characterized by particularly coarse sediment particles. Although grain size data were not available for station 52-C, visual inspection of the sample during treatment revealed high abundance of shell fragments and general coarse texture of the sediment.

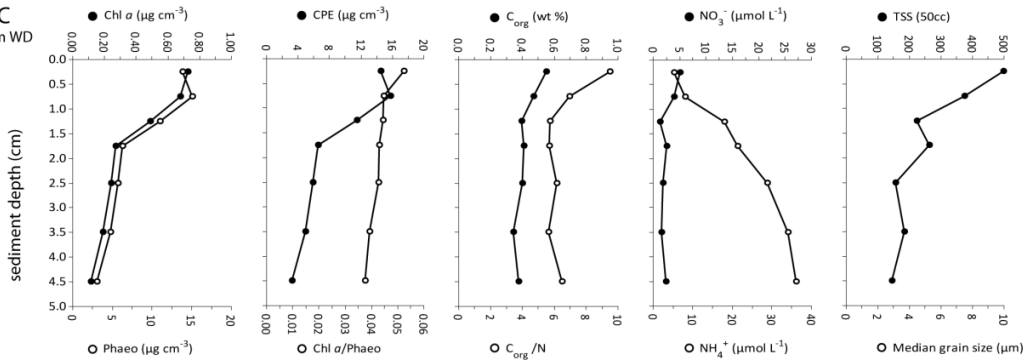
Table 3. Pearson correlation coefficients for the main physical and geochemical parameters, TSS of benthic foraminifera from the >150 µm fraction, TSS of hyaline, porcelaneous agglutinated and arborescent and tubular benthic foraminifera, and diversity (H'). Only top first centimeter values of the environmental parameters are considered in the correlation. For significance level see note below.

	First centimeter										Whole station													
	Water depth	Distance to the shore	CPE	NPD	Median grainsize	Corg	Corg/N	Chl-a	Chl-a/Phaeo	NO ₃	Benthic foraminifera TSS	H'	Hyaline TSS	Porcelaneous TSS	Agglutinated TSS	Arborescent & tubular TSS	Benthic foraminifera TSS	H'	Hyaline TSS	Porcelaneous TSS	Agglutinated TSS	Arborescent & tubular TSS		
NH ₄ ⁺			0.932**					0.937**																
NO ₃ ⁻	0.840**	0.889**									0.847*	-0.913**	0.837*	-0.826**	0.823*		0.761*		0.888*	0.849*				
Chl-a/Phaeo	-0.771*			0.847**							0.768*													
Chl-a			0.996*		0.975**																			
Corg/N						-0.874**																		
Corg																								
Median grainsize											0.992**	0.810**	0.980**	0.968**										
NPD	-0.850**																							
CPE	0.886**	0.908**																						
Distance to the shore																								
Water depth	0.943*										-0.925*	-0.935*	-0.903*	-0.905*										

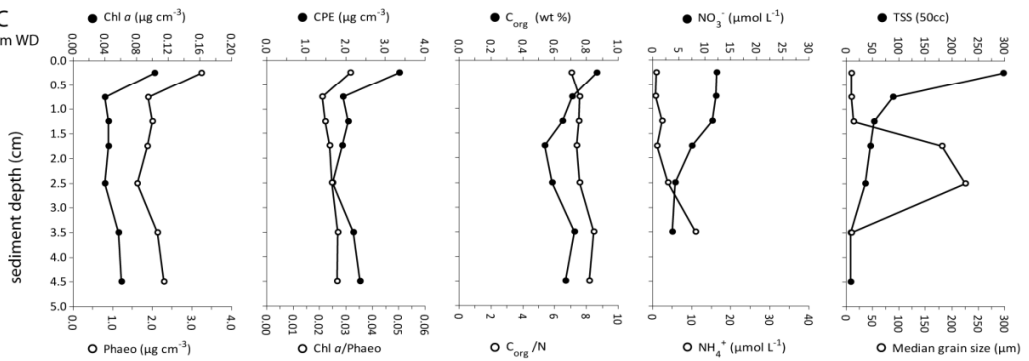
Only significant correlations are shown: in bold p<0.01, in normal font p<0.05 (*N=5, **N=4)

Canyon stations:

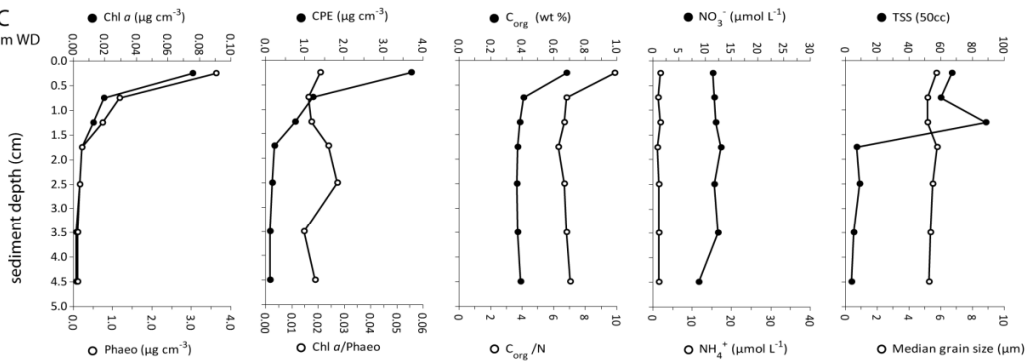
52-C
344 m WD



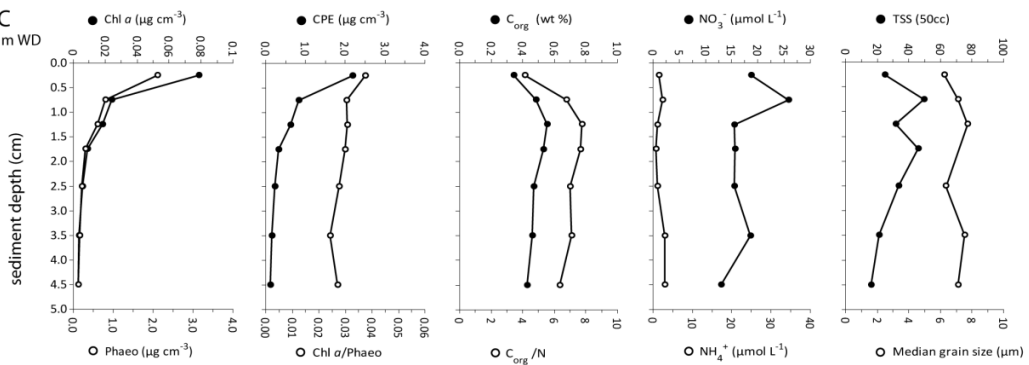
50-C
1215 m WD



47-C
1801 m WD



48-C
2112 m WD



Slope stations:

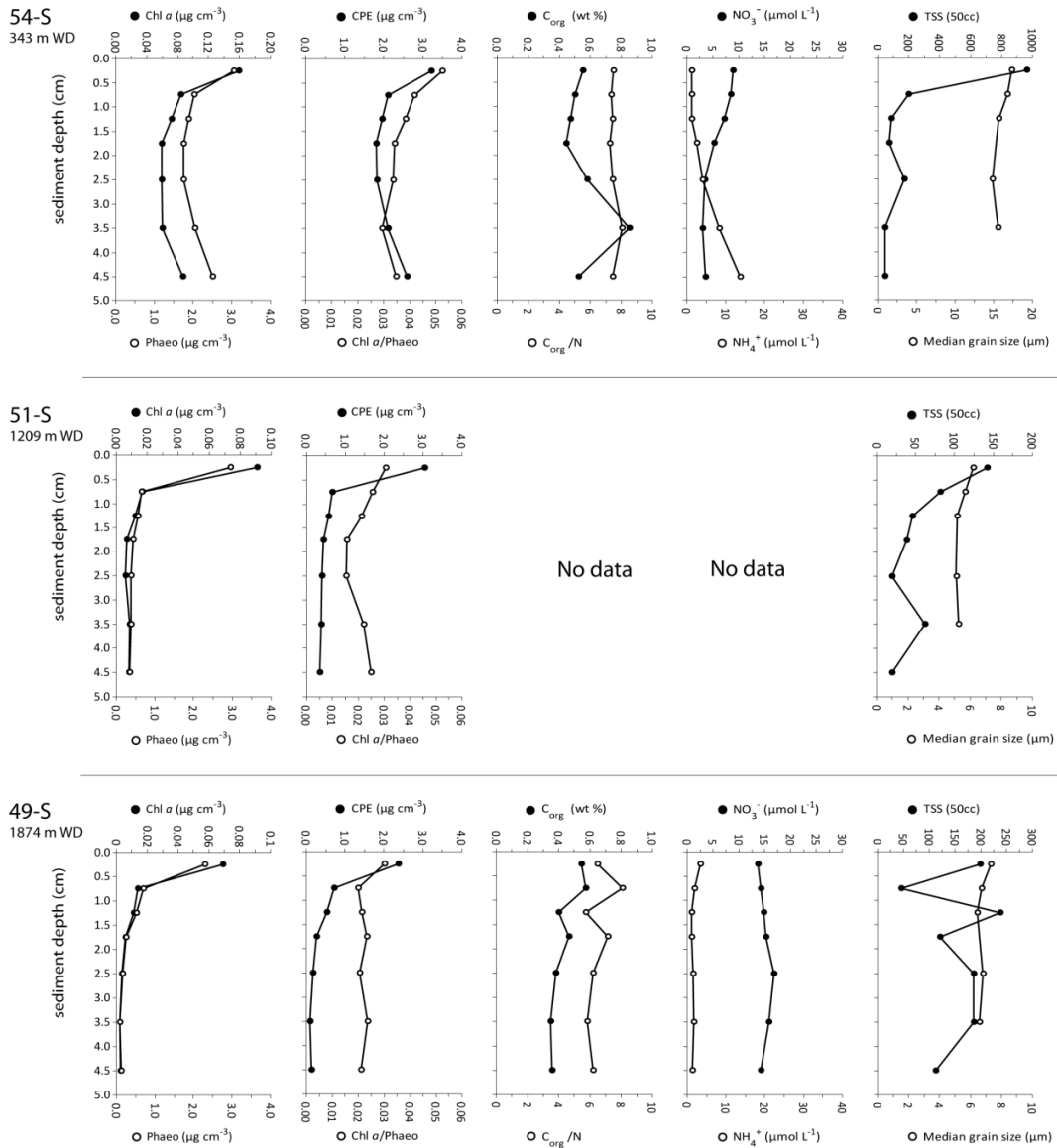


Fig. 4. Down-core profiles of environmental variables: Chlorophyll-a (Chl-a), phaeopigments (Phaeo), chloroplatic pigment equivalents (CPE), chlorophyll-a:phaeopigments ratio (Chl-a/Phaeo), bulk organic carbon (C_{org}), organic carbon:total nitrogen ratio (C_{org}/N), pore water nitrate (NO₃⁻), pore water ammonium (NH₄⁺), and median grain size (note differences in scale bars). Benthic foraminifera total standing stocks (TSS) per station are also plotted. First part of the figure corresponds to canyon stations, second part of the figure corresponds to slope stations. No grain size data available for station 52-C, and no organic carbon, total nitrogen, pore water nitrate and ammonium data are available for station 51-S.

In station 50-C, the presence of a subsurface maximum (between 1.5-5 cm) in median grain size (sand particles up to 225 μm) can be recognized (Fig. 4), while the upper depth levels were characterized by relatively coarse median grain size (fine silt particles between 9-9.6 μm). The shallowest slope station 54-S (343 m WD) displayed median grain size values ranging from 17.3 μm at the surface to 8.7 μm between at 5 cm depth, correspondent with medium to fine silt particles. Station 51-S, at intermediate depths on the slope, presented a finer texture, with median particle size ranging between 5.1 and 6.2 μm , correspondent with fine silt particles. The sediment composition of deeper stations was dominated by fine silt particles, although, a clear trend on the median particle size was not observed either in function of water depth or between canyon and slope environments (results not shown). Station 49-S (1874 m WD) on the open slope, was characterized with larger median grain size (5.7-7.3 μm) than station 47-C (1801 m WD) on the adjacent slope (5.0-5.7 μm); whereas the deepest station 48-C (2112 m WD) was characterized by median grain size values between 6 and 7.7 μm .

Surface median grain sizes displayed a negative correlation with water depth ($P=-0.771$, $p<0.05$), and positive correlation with Chl *a*/Phaeo ratios ($P=0.847$, $p<0.05$) and Chl *a* concentrations ($P=0.975$, $p<0.01$) (Table 3).

4.2 Surface and in-sediment benthic foraminifera distribution

4.2.1 Total Standing Stocks, Diversity and the Average Living Depths of foraminifera

The total standing stocks (TSS) and the proportion of the different benthic foraminifera groups (hyaline, agglutinated, porcelaneous, arborescent and tubular) per station are summarized in Fig. 5. A highly significant negative correlation (Table 4) was found between the top centimeter TSS and increasing water depth. For the whole station, the highest TSS found at the shallowest stations 52-C (657 individuals) and station 54-S (523 individuals). The deep-canyon station 49-S at 1874 m WD, displayed the third highest TSS value from the total analyzed stations (444 individuals). Furthermore, the upper canyon stations generally recorded higher TSS than the adjacent slope stations. This trend was not clear in the lower canyon. Positive correlations were found between median grain sizes and benthic foraminifera TSS ($P=0.982$, $p<0.01$, top-centimeter TSS), and benthic foraminifera TSS and Chl *a*/Phaeo ratios ($P=0.761$, $p<0.05$, whole-station TSS) (Table 3).

At all sites, the communities were dominated by agglutinated foraminifera, followed in abundance by hyaline foraminifera. TSS of hyaline foraminifera had a negative correlation with water depth ($P=-0.959$, $p<0.01$, whole-station TSS; Table 3) and they were higher inside the canyon than on the slope at comparable water depths. Positive correlations were observed between hyaline foraminifera TSS and surficial Chl *a*/Phaeo ratio ($P=0.888$,

$p < 0.01$, whole-sediment TSS) and surficial median grain size ($P = 0.975$, $p < 0.01$, whole-station TSS); whereas a negative correlation was observed with NPD ($P = -0.829$, $p < 0.05$, whole-station TSS) (Table 3). Agglutinated whole-station TSS did not show any obvious trend in relation to the water depth gradient neither for canyon nor slope environments. However, in the top centimeter of sediment, agglutinated foraminifera TSS had a significant positive correlation with surficial median grain size ($P = 0.968$, $p < 0.01$) and surficial Chl *a*/Phaeo ratios ($P = 0.823$, $p < 0.05$), and a significant negative correlation with water depth ($P = -0.905$, $p < 0.01$). Porcelaneous, and arborescent and tubular foraminifera had low abundance within all the communities. Porcelaneous foraminifera whole-station TSS had positive correlation with surficial Chl *a*/Phaeo ratios ($P = 0.849$, $p < 0.05$), surficial CPE concentrations ($P = 0.754$, $p < 0.05$), surficial Chl *a* concentrations ($P = 0.790$, $p < 0.05$) and surficial median grain sizes ($P = 0.913$, $p < 0.05$) (Table 3). Arborescent and tubular foraminifera whole-station TSS had a positive correlation with surficial C_{org} concentrations ($P = 0.939$, $p < 0.01$; Table 3).

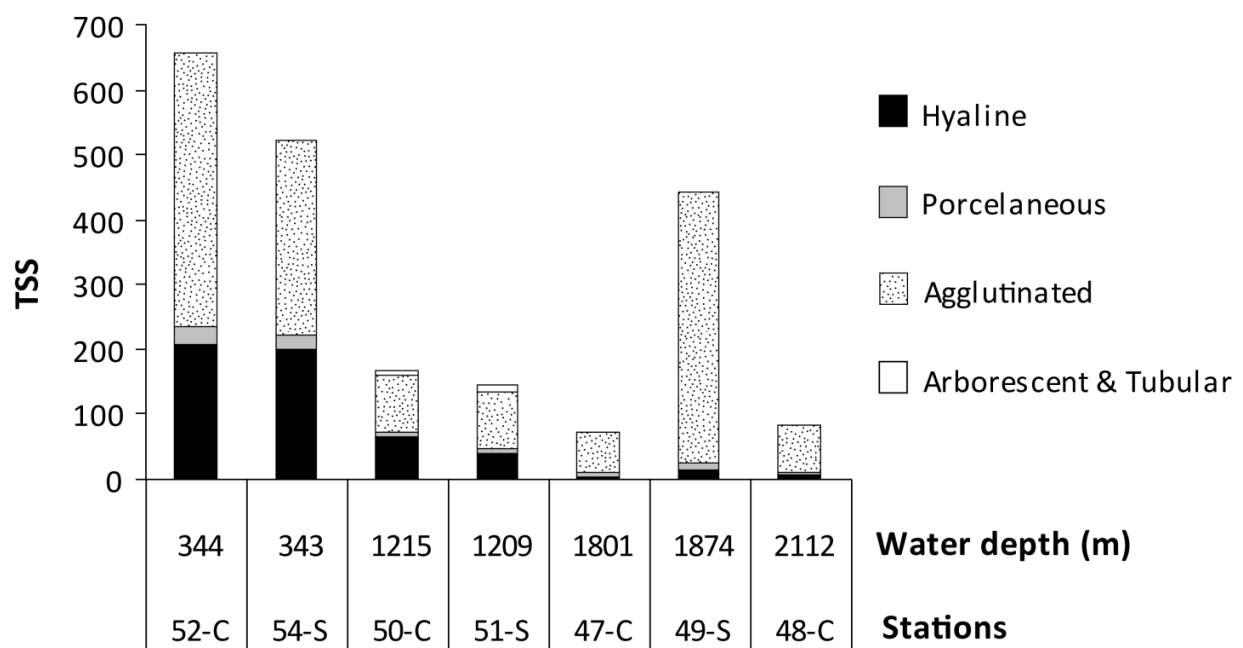


Fig. 5. Total standing stock (TSS) and proportion of benthic foraminifera groups per station. Arborescent and tubular foraminifera abundances are based on individual specimens not fragments. For each station water depth is indicated as well as if they are canyon (C) or slope (S) stations. Stations arranged in increasing water depth.

Diversity values for each station are presented in Table 4. The highest number of species ($S = 74$) as well as the highest diversity ($H' = 3.271$) were found at the station 52-C. In general, the number of species and diversity decreased with increasing water depth (Fig 3B) with which a highly significant negative correlation was observed for the top centimeter of sediment (Table 3).

Table 4. Total standing stocks (TSS), average living depths (ALD), species number (S) and Shannon diversity index (H') of benthic foraminifera per station. TSS and ALD are also presented for the different benthic foraminiferal groups. ALD for arborescent and tubular foraminifera were not included since they grow through different sediment levels.

Station	TSS	ALD	NPD	S	H'	Hmax	E	Hyaline		Porcelaneous		Agglutinated		Arborescent & tubular	
								TSS	ALD	TSS	ALD	TSS	ALD	TSS	ALD
52-C	657	1.39	0.50	74	3.271	4.304	0.760	208	1.37	27	0.63	421	1.42	1	
54-S	523	1.10	2.25	65	3.109	4.174	0.745	198	0.76	23	1.38	301	1.36	1	
50-C	167	1.48	2.50	53	3.147	3.970	0.793	66	1.63	7	0.70	87	1.49	7	
51-S	144	1.44		36	2.721	3.584	0.759	41	0.85	6	2.41	89	1.58	8	
47-C	73	0.81	6.50	19	2.020	2.944	0.686	4	1.33	8	1.03	61	0.64		
49-S	444	1.11	11.00	33	1.110	3.497	0.318	16	1.01	11	1.65	415	1.00	2	
48-C	83	1.13	8.75	18	1.585	2.890	0.548	6	0.75	6	1.40	71	1.07		

This decrease trend was observed in, both, canyon and slope stations. Station 49-S was an exception since the number of species was about one and a half times higher than at stations located at similar water depth, although its diversity (H') was the lowest registered from all stations. The canyon stations displayed higher diversity values than stations in the slope at comparable depths. Evenness values were the highest at station 50-C ($E= 0.793$) followed by station 52-C ($E= 0.760$), and for the rest of the stations the usual inverse relationship with water depth was observed. Canyon stations have higher evenness than slope stations at comparable depth. Whole-station diversity values displayed a highly significant negative correlation with NPD (Table 3).

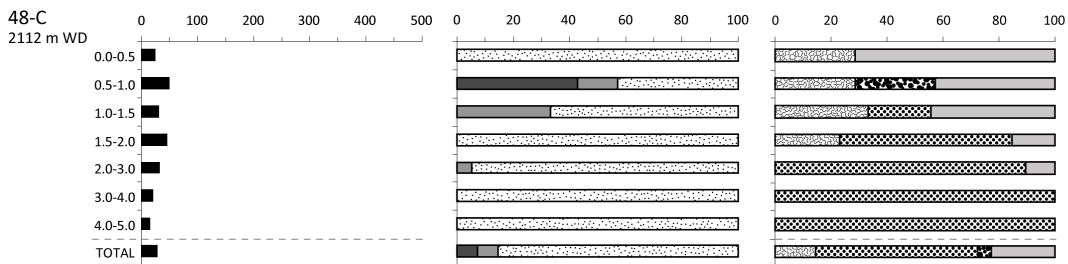
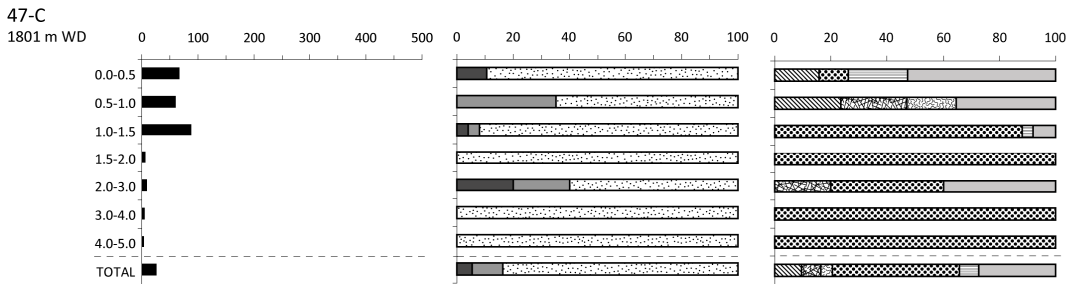
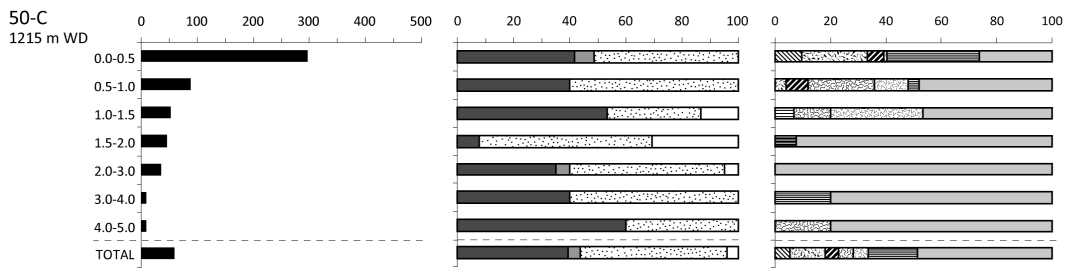
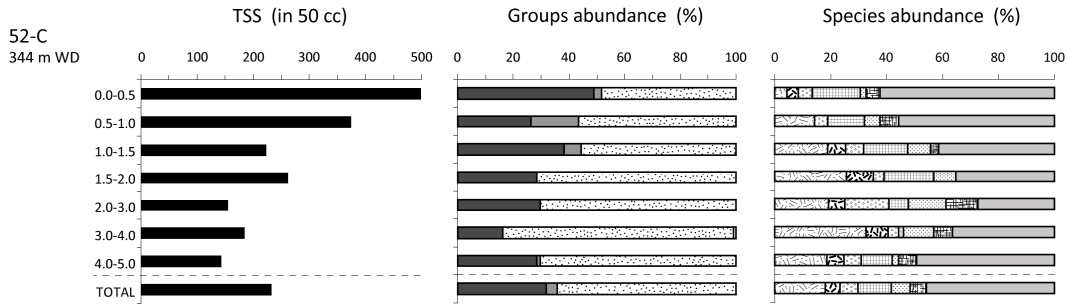
The average living depths (ALD) of the foraminiferal communities ranged between 0.81 and 1.48 cm (Table 4). The ADL did not show a clear pattern with respect to water depth. The deepest ALD occurred on the middle-depth canyon station 50-C (at 1215 m WD), followed by station 51-S (at 1209 m WD with 1.44 cm). Hyaline foraminifera presented deeper ALD in canyon stations than porcelaneous foraminifera (except in station 48-C), and vice versa for the slope stations. The ALD of agglutinated foraminifera did not show any particular trend, either with water depth of between canyon and slope environments.

4.2.2. Down-core species distribution, group abundances and species assemblages

In Fig. 6 the TSS per sediment depth level, the abundance of the different groups of foraminifera and the abundance of the most frequent foraminiferal species (>4% of the TSS) of the seven stations in the Cap de Creus Canyon and adjacent slope are presented. In general, the TSS decreased with increasing sediment depth, with exception of station 49-S, in which a subsurface maximum can be observed around 1.0-1.5 cm. Station 52-C had the highest TSS at almost all sediment depth levels, it was, followed by stations 49-S and 54-S. Station 54-S had a significantly higher core top TSS in comparison to the other stations, which was twice as high as the core top TSS for station 52-C.

The relative abundance of agglutinated foraminifera showed no clear trend with sediment depth, but they usually presented a relative abundance subsurface maximum. Hyaline foraminifera were more abundant and had deeper penetration into the sediments in canyon shallow stations; their in-sediment abundance decreased in the open slope and deeper stations. An exception was station 48-C which presented a subsurface maximum at the 0.5-1.0 level. Porcelaneous foraminifera displayed low abundances towards the sediment surface; however, in some cases they increased their abundance at deeper levels in the sediment. Their maximum abundances occurred at shallow slope stations between 1.5-5.0 cm, and at deep canyon stations between 0.5-3.0 cm.

Canyon stations:



Foraminifera groups

- Hyaline
- Porcelaneous
- Agglutinated
- Arborescent & tubular

Foraminifera species

- *Ammoscalaria pseudospiralis*
- *Bigenerina nodosaria*
- *Bulimina aculeata*
- *Cibicides ungerianus*
- *Spiroplectinella sagittula*
- *Textularia agglutinans*
- *Ammolagena clavata*
- *Crithionina* cf. *C. mamilla*
- *Discammina compressa*
- *Glomospira charoides*
- *Melonis barleeanus*
- *Uvigerina mediterranea*
- *Cruciloculina* cf. *C. triangularis*
- *Haplophragmoides* sp. (coarse grains)
- Agglutinated dome
- *Gyroidinoides soldanii*
- Rest

Slope stations:

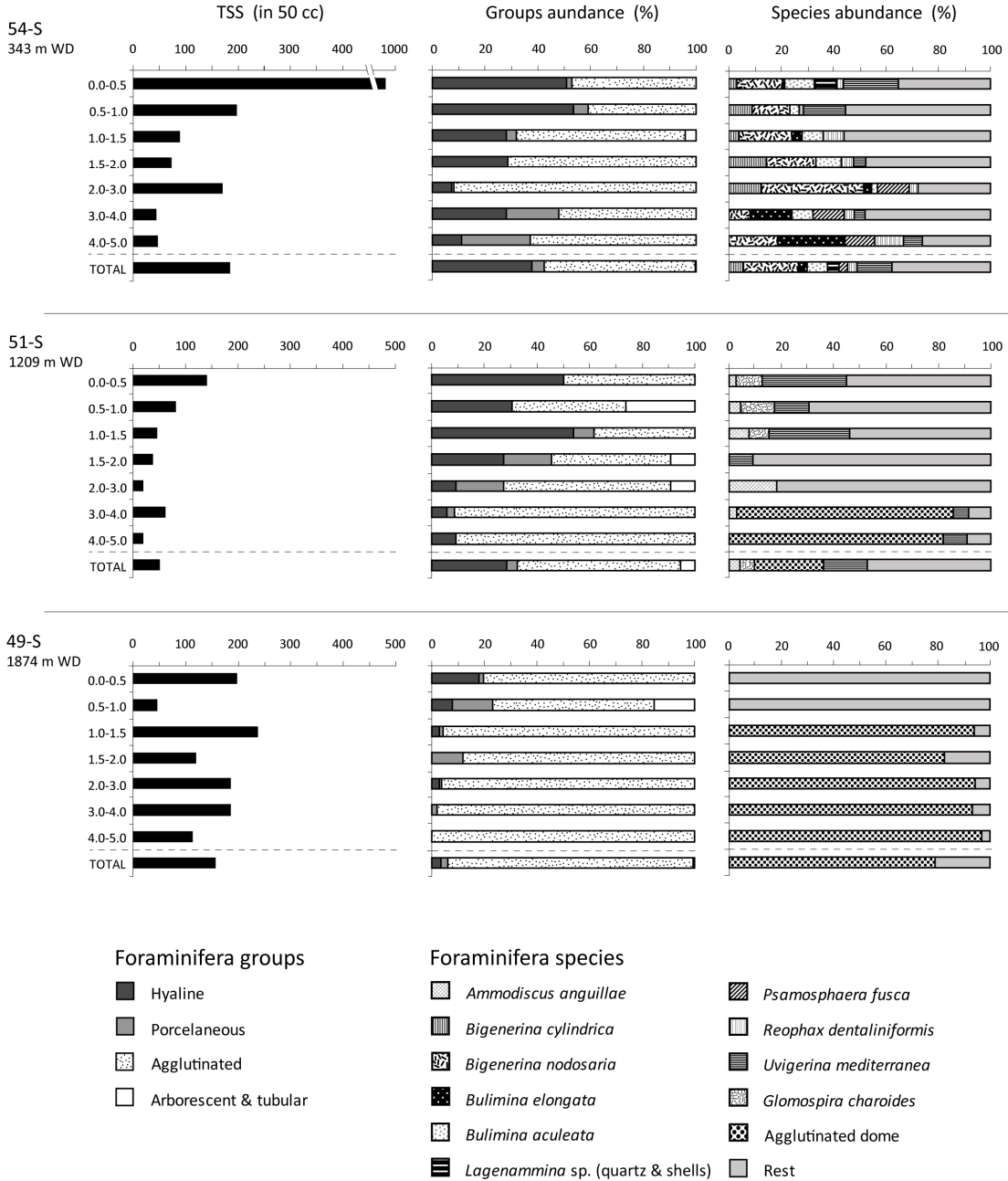


Fig. 6. Benthic foraminifera distribution in sediment. Data correspond to the >150 μm fraction counts. Left panels: Total standing stocks (TSS) are standardized for 50 cubic centimeters (50 cc); stations totals are also standardized for 50 cc (note the different scale bars). Central panels: Main benthic foraminifera groups abundances. Right panels: Relative abundance for all species accounting for more than 4 % of TSS per sediment level. The first part of the figure corresponds to canyon stations, the second part of the figure corresponds to slope stations.

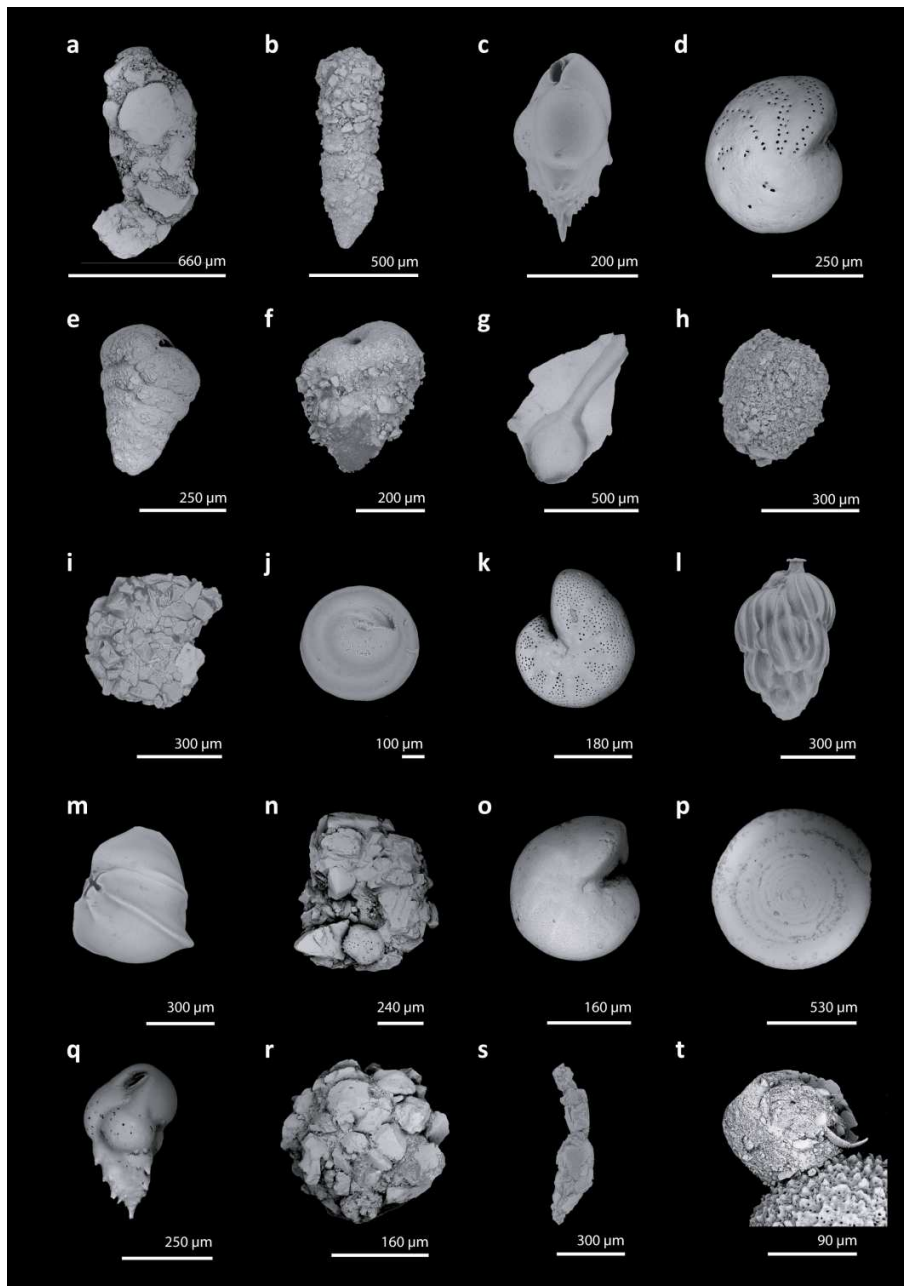


Plate 1. Common benthic foraminifera species in the >150 μm fraction. (a) *Ammoscalaria pseudospiralis*, station 52-C (0-0.5 cm); (b) *Bigenerina nodosaria*, station 54-S (0-0.5 cm); (c) *Bulimina aculeata*, station 54-S (0-0.5 cm); (d) *Cibicides ungerianus*, umbilical side, station 52-C (0-0.5 cm); (e) *Spiroplectinella sagittula*, station 52-C (0-0.5 cm); (f) *Textularia agglutinans*, station 54-S (0-0.5 cm); (g) *Ammolagena clavata*, station 50-C (0-0.5); (h) *Chrithionina* cf. *C. mamilla*, station 50-C (0-0.5 cm); (i) *Discammina compressa*, station 50-C (0-0.5 cm); (j) *Glomospira charoides*, apertural view, station 51-S (0-0.5 cm); (k) *Melonis barleeanus*, lateral view, 50-C (1-1.5 cm); (l) *Uvigerina mediterranea*, 54-S (0-0.5 cm); (m) *Cruciloculina* cf. *C. triangularis*, apertural view, station 50-C (0-0.5 cm); (n) *Haplophragmoides* sp. "coarse grains", station 47-C (0-0.5 cm); (o) *Gyroidinoides soldanii*, umbilical side, station 50-C (1-1.5 cm); (p) *Ammodiscus anguillae*, station 51-S (0-0.5 cm); (q) *Bulimina elongata*, station 54-S (3-4 cm); (r) *Psamosphaera fusca*, station 47-C (0.0.5 cm); (s) *Reophax dentaliniformis*, station 54-S (0-0.5 cm); (t) "Agglutinated dome" incrusting on a planktonic foraminiferal test, station 49-S (3-4 cm).

Assemblages changed between canyon and slope environments, and between shallow and deep stations (Fig 4). The canyon head station 52-C (344 m WD) displayed an assemblage dominated by *Ammoscalaria pseudospiralis* (17.96 %) together with *Cibicides ungerianus* (11.87 %). Other abundant species in this station were *Spiroplectinella sagittula* (6.84 %), *Bulimina aculeata* (6.39 %), *Textularia agglutinans* (5.78 %) and *Bigenerina nodosaria* (5.32 %). The station 54-S (343 m WD), located on the slope, displayed a different species assemblage, dominated by the species *Bigenerina nodosaria* (21.03 %) and *Uvigerina mediterranea* (13.38 %). Other important species were *Bulimina aculeata* (7.83 %), *Bigenerina cylindrical* (5.54 %), *Lagenammina* sp. (quartz & shells) (4.39 %), *Psamosphaera fusca* (3.44 %) and *Reophax dentaliniformis* (3.44 %).

At the canyon station 50-C (1215 m WD) the most abundant taxa were *Uvigerina mediterranea* (17.96 %) and *Crithionina* cf. *C. mamilla* (12.57 %); other abundant species were *Melonis barleeanus*, *Glomospira charoides* and *Ammolagena clavata* (each one of them with 5.38 %) and *Discammina compressa* (4.79 %). Located on the open slope, station 51-S (1209 m WD) was dominated by a single-chambered unidentified “agglutinated dome” species (26.38 %; see Plate 1) and *Uvigerina mediterranea* (16.66 %). Another two abundant species were *Glomospira charoides* (5.55 %) and *Ammodiscus anguillae* (4.16 %).

At station 47-C, the shallowest station of the lower canyon section (1801 m WD), had an assemblage dominated by the “agglutinated dome” species (45.20 %); four other species also presented relatively high abundance: *Ammolagena clavata* (9.58 %), *Cruciloculina* cf. *C. triangularis* and *Haplophragmoides* sp. (coarse grains) (both 6.84 %) and *Glomospira charoides* (4.10 %). In station 49-S (1874 m WD), located on the slope, the “agglutinated dome” species accounted for 78.82 % of the total standing stock and was the only species with a total relative abundance higher than 4%. The “agglutinated dome” usually displayed its maximum abundance in the subsurface and low surface abundances. Station 48-C located at the most distal part of the canyon (2112 m WD) also displayed an assemblage dominated by the “agglutinated dome” (57.83 %), but together with other two species: *Glomospira charoides* (14.45 %) and *Gyroidinoides soldanii* (4.81 %).

4.2.3. The arborescent and tubular agglutinated foraminifera

The arborescent and tubular foraminifera were counted as individuals in the presence of a terminal bulb or middle bulge (as in Koho et al. 2007); however large amounts of fragments of these organisms containing stained cytoplasm were present in the samples which were qualitatively quantified Fig. 7.

The highest abundance of fragments occurred at station 50-C at the upper canyon section, where *Dendrophrya* sp. and *Saccorhiza ramosa* were most abundant. The second largest number of fragments occurs at station 51-S

located at the slope at similar depth than station 50-C. Here, the most abundant species are *Hyperammina elongata* and also *Saccorhiza ramosa*. Shallow stations (52-C and 54-S) presented few fragments in general, in particular at the canyon head. Species of the genus *Hyperammina*, as well as *Bathysiphon* were found around these depths in low abundances. At the upper canyon section (station 50-C) and adjacent slope (station 51-S) other species were also found, such as *Rhabdammina linearis*, *Hyperammina elongata*, *Jacullella acuta*, *Botellina labyrinthica*, *Bathysiphon capillare*, *Bathysiphon filiformis* and *Bathysiphon rufus*. At the lower canyon section, fragments of *Saccorhiza ramosa* were usually the most abundant; however fragments of *Hyperammina elongata* and *Dendrophrya* sp. were also found in low abundances. In contrast, station 48-C was totally deprived of fragments. Overall, the arborescent and tubular foraminifera (including the fragments, as well as bulbs and bulges) occurred exclusively in the top 2 cm of sediment, with now occurrences registered beneath this depth.

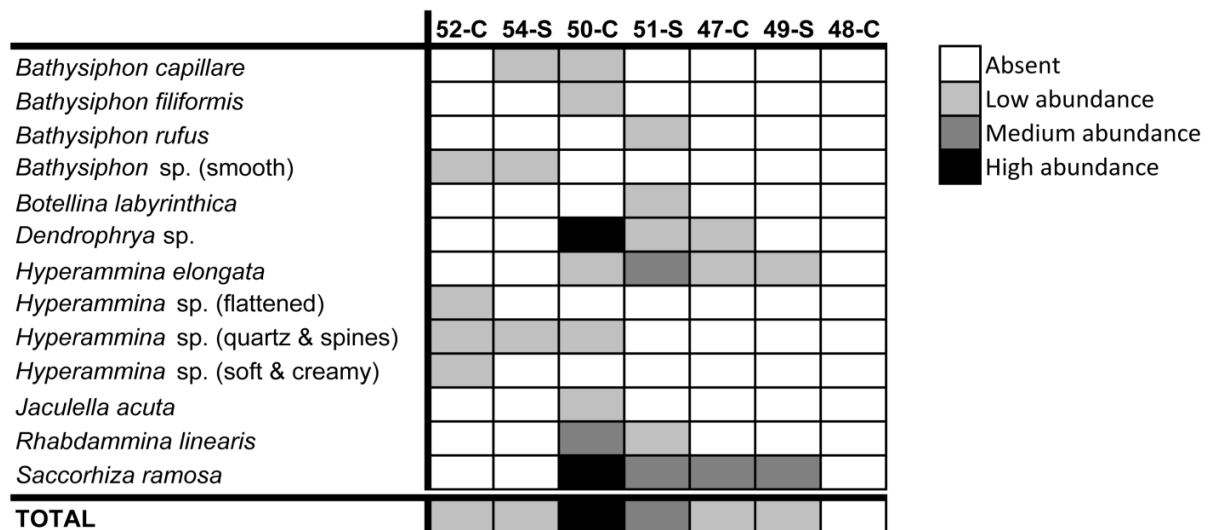


Fig. 7. Qualitative estimation of abundance of arborescent and tubular benthic foraminifera per station. The gray color scale is based on the number of fragments per species in every station. The total refers to the number of fragments of all arborescent species per station.

4.2.4. The core top 63-150 μm fraction benthic foraminifera

The comparison between the large (>150 μm) and small (63-150 μm) fractions was considered important as several species can be underrepresented in the large fraction (Fig. 8A). Generally in the core top samples, the TSS of small foraminifera was higher than the large foraminifera. However, the Shannon index (H') value was higher for the >150 μm fraction at the canyon head (station 52-C) and also at the lower canyon and slope area (stations 47-C and

49-S). Evenness was usually higher in the >150 μm fraction with the exception of stations 54-S and 50-C in which it was higher in the 63-150 μm fraction. It is worth to notice that for the 63-150 μm fraction, TSS values do not show a specific trend in response to water depth, however diversity (Shannon index value and number of species) does. The abundant (> 1 %) benthic foraminifera species observed in the 63-150 μm fraction of the core top samples are presented in Fig. 8B.

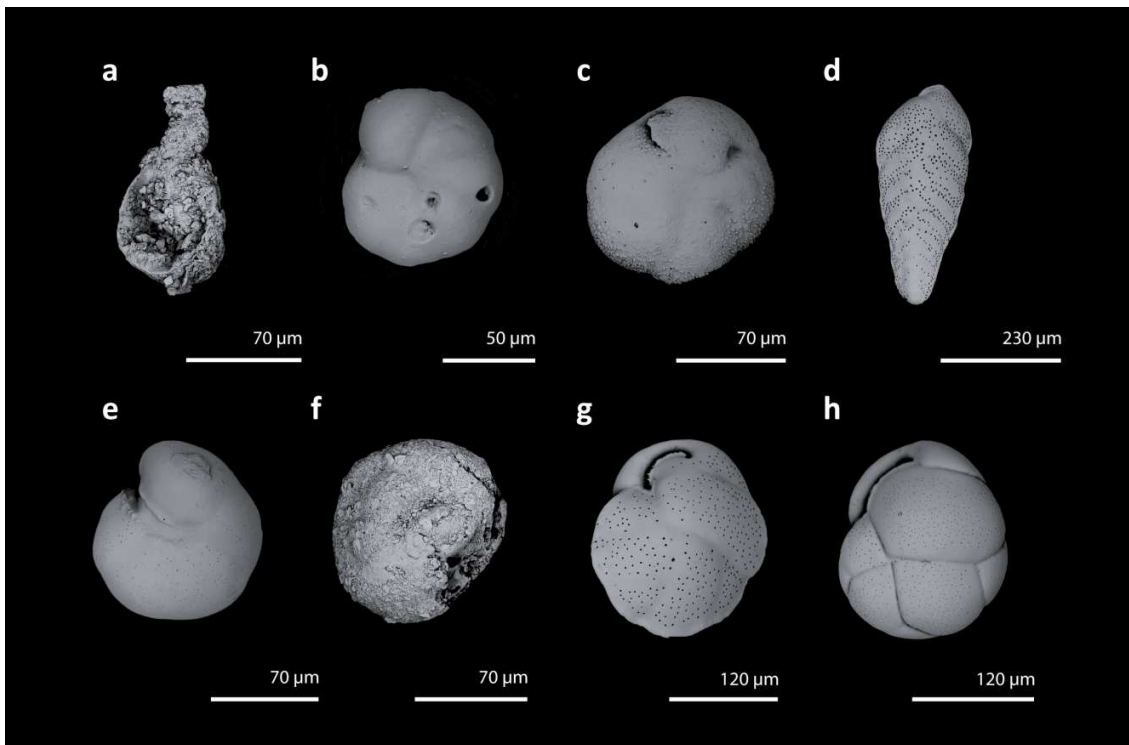


Plate 2. Common benthic foraminifera species in the 63-150 μm fraction. (a) *Lagenammina* sp. "organic wall", station 49-S (0-0.5 cm); (b) *Pseudoparella* sp., umbilical side, station 49-S (0-0.5 cm); (c) *Eponides pusillus*, umbilical side, station 51-S (0-0.5 cm); (d) *Bolivina spathulata*, station 52-C (0-0.5 cm); (e) *Gyroidinoides umbonatus*, umbilical side, station 47-C (0-0.5 cm); (f) *Glomospira* sp. "white", station 48-C (0-0.5 cm); (g) *Cassidulina laevigata*, umbilical side, station 52-C (0-0.5 cm); (h) *Cassidulina crassa*, umbilical side, station 52-C (0-0.5 cm).

At the canyon head station (52-C), the small fraction was dominated by *Bolivina spathulata* and *Cibicides* spp. (from which most of them probably belong to *C. ungerianus*; however species identification was not always possible due to the young ontogenetic stage). Other abundant species in this station were *Cassidulina laevigata*, *Cassidulina crassa*, *Bulimina aculeata* and *Glomospira* sp. (white). At similar water depth on the slope the assemblages were dominated by *B. nodosaria* and *B. spathulata*. Other abundant species were *Lagenammina difflugiformis*, *Saccamina* sp. (white & smooth), *C. laevigata*, *C. crassa* and *Trochammina globigeriniformis*.

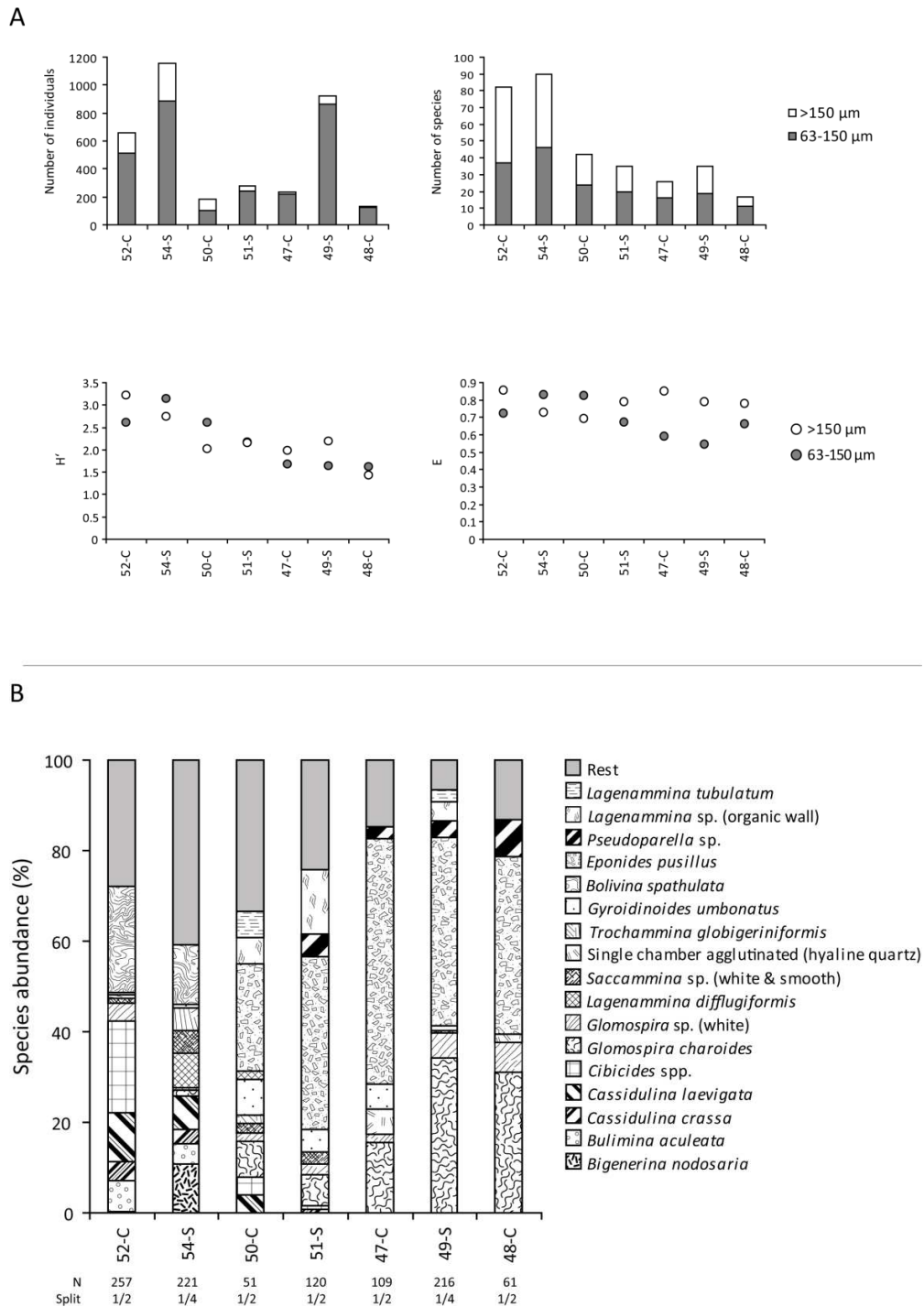


Fig. 8. (A) Comparison between the 63-150 μm and the >150 μm fractions in core top samples of all stations. The abundances of foraminifera in the 63-150 μm splits were extrapolated to abundances for the whole sample. Raw abundances values are presented for both fractions (values not standardized to 50cc). The two fractions are compared in terms of number of individuals (N), number of species (S), Shannon diversity index (H') and evenness (E). (B) Relative abundance of species accounting for more than 1% of the TSS of 63-150 μm . The total number of individuals per sample is indicated (N) as well as the split that was analyzed.

The most common species at the upper canyon station (50-C) were *Eponides pusillus*, *G. charoides* and *Gyroidinoides umbonatus*; other abundant species were *Lagenammina tubulatum*, *Lagenammina* sp. (organic wall), *Cibicides* spp. and *C. crassa*. On the corresponding slope station the assemblage becomes clearly dominated by *E. pusillus*. Other abundant species were *Lagenammina* sp. (organic wall), *G. charoides*, *G. umbonatus* and *Pseudoparrella* sp. In the lower canyon and slope stations (47-C, 49-S and 48-C) the faunas were mostly composed of *E. pusillus* and *G. charoides*. Other relatively common species were *Pseudoparrella* sp., *G. umbonatus*, *Glomospira* sp. (white), *Lagenammina* sp. (organic wall) and a single-chambered agglutinated unidentified species.

4.3. Environmental parameters and benthic foraminifera distribution: the TROX (Trophic-Oxygen) model

In order to investigate the way in which food and redox chemistry determine the benthic foraminiferal distribution in the Cap de Creus canyon and adjacent slope, a trophic oxygen map (TROX map) was constructed on the basis of the vertical concentration profiles of CPE (as indicator of food abundance) and NO_3^- (as indicator of redox chemistry) (Fig. 9A). Nitrate concentrations in station 51-S were interpolated from values of stations 50-C and 47-C since pore water data for this station were not available. In this map, all the stations were organized along a CPE- NO_3^- gradient in which sedimentary CPE concentrations decreases while the penetration depth of pore water NO_3^- increases, in other words the gradient reflects a change from eutrophic to oligotrophic conditions. The objective of this exercise was to rank the stations according to their trophic state and to identify the responses of selected species to the trophic state of the environment. The selected species were chosen because they are frequently reported in studies focused on benthic foraminiferal response under different productivity regimes, and because they were abundant in the samples.

Environments with high surface CPE concentrations $>5 \mu\text{g cm}^{-3}$ (Fig. 9B) were dominated by *A. pseudospiralis*, *C. ungerianus*, and *S. sagittula*, whose in-sediment distribution appeared to be limited by the CPE concentration ($>3 \mu\text{g cm}^{-3}$ isoline). These species displayed shallow to intermediate infaunal habitats along the isolines with increasing abundances towards areas with high CPE concentration ($>5 \mu\text{g cm}^{-3}$). From all the species, *A. pseudospiralis* recorded the highest abundances deep in the sediment and within the anoxic zone. In the border of high CPE concentration ($>5 \mu\text{g cm}^{-3}$) environments was *B. nodosaria*, which presented its maximum abundance in the edge between the oxic and dysoxic zones (pore water NO_3^- concentrations $\sim 8 \mu\text{mol L}^{-1}$) with a second subsurface maximum within the anoxic zone (pore water NO_3^- concentrations $<4 \mu\text{mol L}^{-1}$). This species had its highest abundances in areas of intermediate food availability (in-sediment CPE concentrations $2-5 \mu\text{g cm}^{-3}$) and displayed

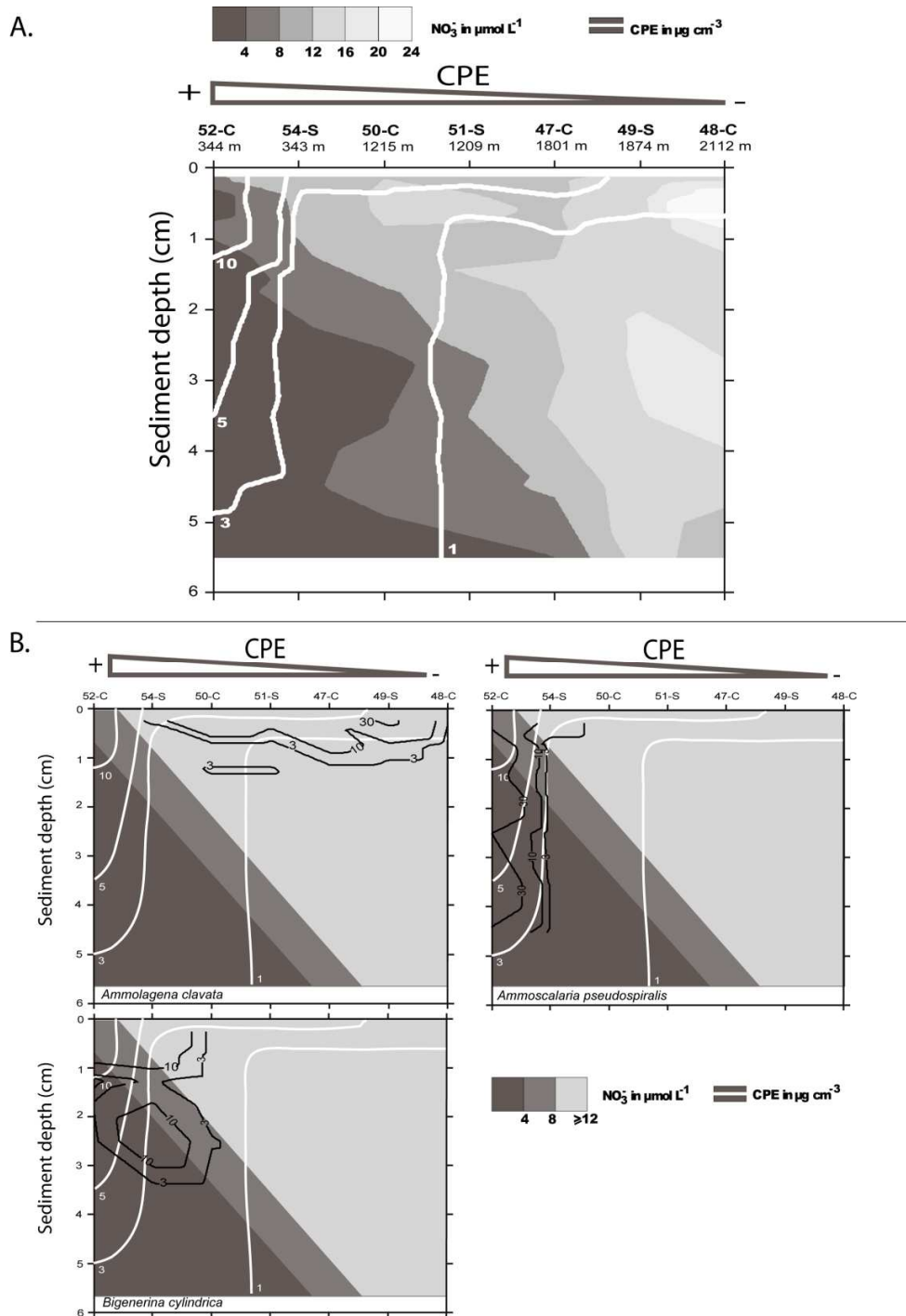
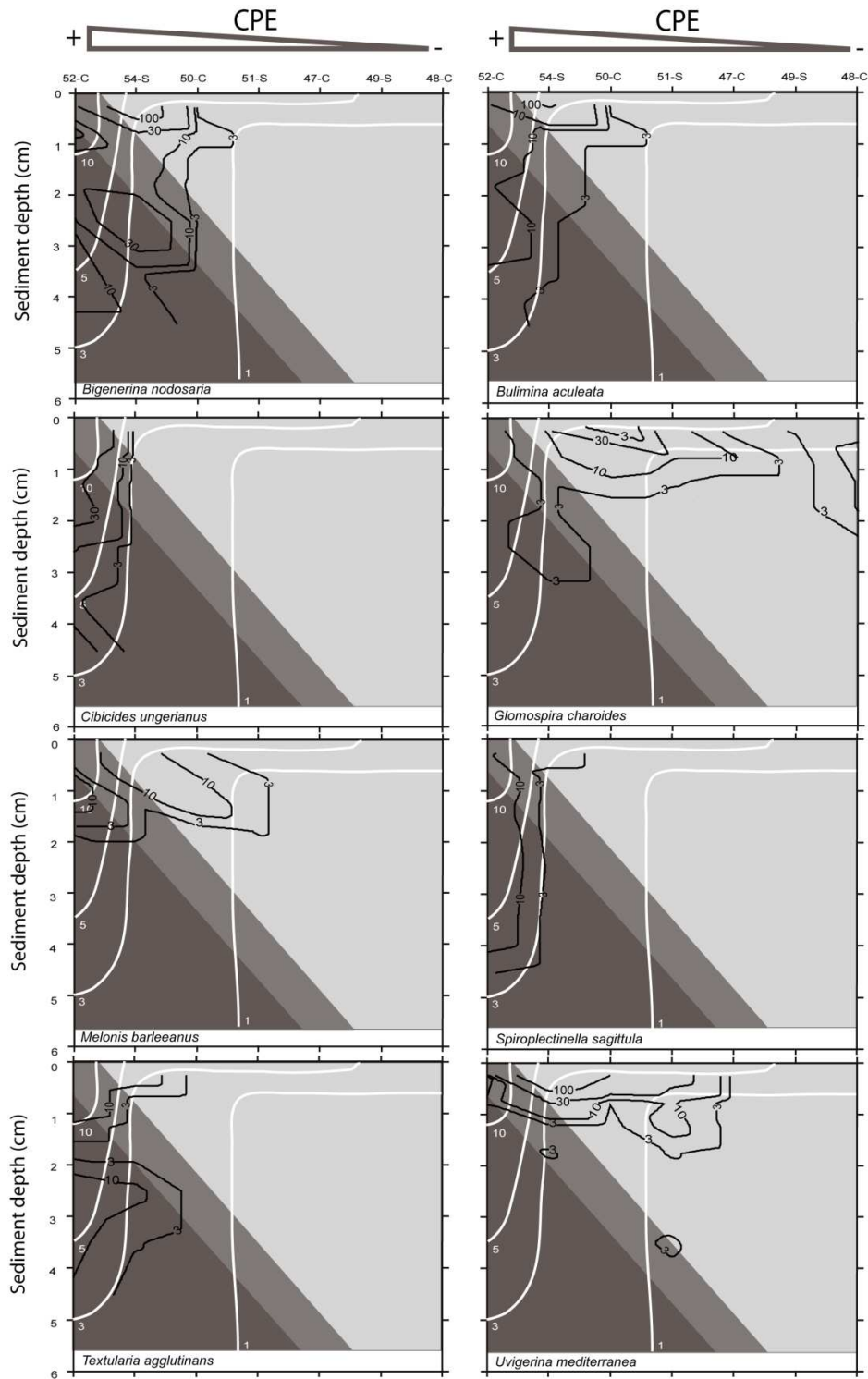


Fig. 9. (A) CPE and pore water nitrate (NO₃⁻) matrix along a gradient of decreasing CPE concentration in the top 5 cm of sediment. Stations are arranged according to decreasing values of CPE concentration; however, the gradient also coincides with increasing water depth. Higher CPE concentrations correspond with in-sediment nitrate depletion indicating eutrophic conditions. (B) Contour plots of in-sediment distribution of selected benthic foraminifera species. The counts are standardized for 50 cc. Pore water nitrate and CPE concentrations in the sediment are schematized. Single foraminifera occurrences were not



included. Light-gray area represents well oxygenated oligotrophic environments, middle-gray area represents the denitrification zone in the sediment where nitrate starts being consumed for respiration instead of oxygen (dysoxic conditions), dark-gray area represents sediments below denitrification zone considered anoxic.

shallow to intermediate infaunal habitats. Other species associated with intermediate to high surface CPE concentrations ($3-10 \mu\text{g cm}^{-3}$) were *U. mediterranea*, *B. aculeata*, *T. agglutinans*, *M. barleeanus* and *B. cylindrica*. The last two species are found in the dysoxic nitrate reduction zone. In particular, *B. aculeata* and *B. nodosaria* had maximum abundances in the edge between the oxic and dysoxic areas (pore water NO_3^- concentrations $\sim 8 \mu\text{mol L}^{-1}$); although *B. aculeata* extended, with progressively decreasing abundances, deeper into the anoxic zone. *U. mediterranea*, was never found within the anoxic zone and had maximum abundances within oxic sediments. Habitats with surface CPE concentrations $< 2 \mu\text{g cm}^{-3}$ were dominated by the species *A. clavata*, which occupied a shallow infaunal habitat. Finally, *G. charoides* was usually constrained into oxic surface sediments with maximum abundances in habitats of intermediate surface CPE concentration ($\sim 3 \mu\text{g cm}^{-3}$) but also occupying habitats with low CPE surface concentrations ($< 2 \mu\text{g cm}^{-3}$).

4.4 Environmental control on the spatial distribution of benthic foraminifera

The detrended correspondence analysis (DCA; Fig 10) was used as an approach to characterize canyon and slope environments in function of their benthic foraminifera distribution and geochemical parameters. In the analysis, variance was explained by four main axes; the first axis explained 51.6 % of the total variance, whereas the second axis explained 20 % of the total variance. The third axis explained 3 % of the total variance and the fourth axis represented 0.3 % of the total variance. Together, the first and the second axes explained 71.6 % of the total variance.

DCA axis 1 aligned closely with the Chl *a*/Phaeo ratio and water depth, and thus appears to represent the decreasing proportion of chlorophyll *a* with respect to the phaeopigments with increasing water depth. DCA axis 2 aligned with the canyon and slope environment vector as well as with the CPE concentrations, the CPE and canyon vector pointing in the same direction. All these factors (Chl *a*/Phaeo ratio, water depth, CPE concentration and canyon or slope location) seemed to be the most important drivers of the distribution of benthic foraminifera in the Cap de Creus canyon and slope area since all the species respond to one or the other axis.

The analyzed stations were plotted on the DCA diagram in function of their benthic foraminiferal assemblages and environmental characteristics. Shallow stations aligned well with canyon or slope trends, as it can be seen in the opposite location of stations 52-C and 54-S along DCA axis 2. Stations at deeper areas presented a more neutral position along DCA axis 2, suggesting less clear trends between canyon and slope environments, as it can be observed for stations 47-C, 49-S and 48-C.

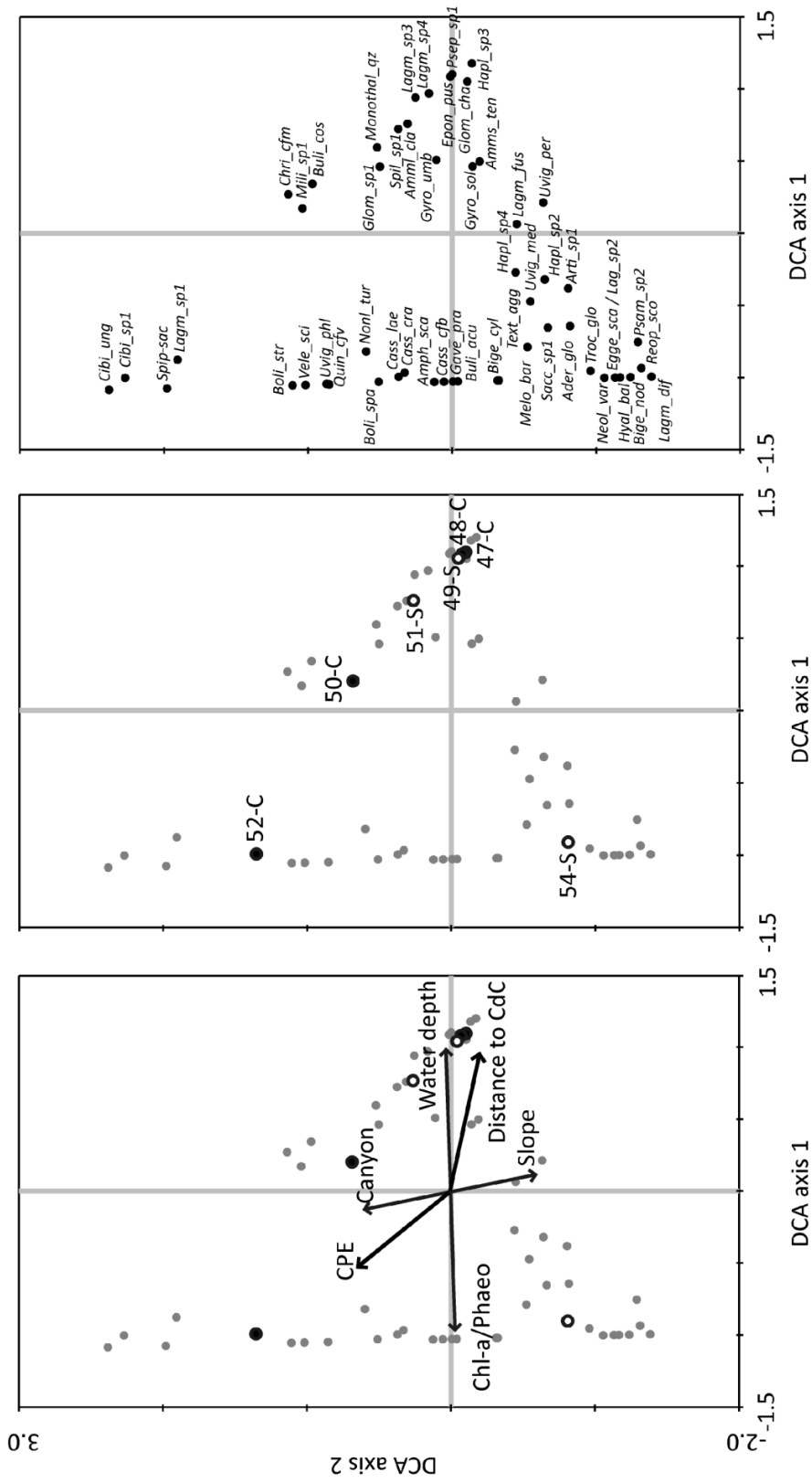


Fig. 10. Detrended correspondence analysis (DCA) showing the relationship between environmental parameters and benthic foraminifera species abundances using the second order polynomial detrending method. The analysis classifies the stations according to their environmental characteristics and plots the species in agreement to their ecological preferences. Axes 1 and 2 explain together 71.6 % of the total variance. Benthic foraminifera species were selected from both the 63-150 μm and the >150 μm fractions, rare species were excluded.

5. Discussion

5.1 Canyon versus open slope: benthic environments as a function of food quantity and quality

Organic carbon, either fluxes or sedimentary content, is commonly used as an indicator of the trophic state of marine environments (de Rijk et al., 2000; Jorissen et al., 2007; Licari and Mackensen, 2005; Schmiedl et al., 2000). However, our results pointed out that bulk C_{org} content had no obvious correlation with water depth and no substantial differences were observed between canyon and slope environments (Fig. 3A). In contrast to the bulk C_{org} content, CPE concentration and Chl a /Phaeo ratio had an inverse correlation with water depth (Fig. 3A) which was significant at the 5% level for the Chl a /Phaeo ratio ($P=-0.771$; Table 4). In the same line, the TSS displayed significant positive correlation with the Chl a /Phaeo ratio ($P=0.847$, $p<0.05$), whereas diversity (H') displayed a significant positive correlation with Chl a concentration in the sediments ($P=0.768$, $p<0.05$) (Table 3). This evidence supports the idea that phytopigments are more important in determining the food availability for benthic foraminiferal communities than bulk organic carbon; an observation previously made by Koho et al. (2008) for the Lisbon-Setúbal canyon. This is because phytopigments represent the labile fraction of organic matter and therefore the freshest and easily degradable food source, whereas bulk organic carbon accounts for the total organic matter deposited, including partially degraded organic matter and also refractory organic matter.

Sediment surface phytopigment concentrations (CPE) were always higher inside the canyon than on the open slope at comparable water depths (Fig. 3A). Values were particularly high at station 52-C ($15.15 \mu\text{g cm}^{-3}$) in comparison to station 54-S ($2.65 \mu\text{g cm}^{-3}$). However, surficial Chl a /Phaeo ratios became higher on the open slope with increasing water depth than inside the canyon (Fig. 3A). Stations 52-C and 54-S, which displayed the largest difference in CPE concentrations, showed very similar Chl a /Phaeo ratio values (0.0484 and 0.0481 respectively). Reworking of labile organic matter during its transport down-canyon probably accelerates its degradation, while it also causes dilution of fresh labile organic matter deposited *in situ* with degraded labile organic matter transported from up-canyon. In general, the Chl a /Phaeo ratio values decrease towards deeper stations, with the noticeable exception of station 48-C (ratio value of 0.035). Therefore, DSWC contributes to increase labile organic matter deposition inside the canyon but also increases its degradation through reworking. The reach of influence of the DSWC is unclear, although it seems to be restricted to the canyon head and the upper canyon. Sánchez-Vidal et al. (2009) were able to track the down-slope transport of chlorophyll-rich shelf waters in the form of a 200-500 m thick layer with increased fluorescence inside the Cap de Creus canyon at >1500 m WD in April 2006. Their observation evidences that even in strong DSWC years the lower canyon is rarely affected.

García et al. (2008) calculated Chl *a* deposition rates on the same samples analyzed in our study, with the exception of the canyon head. Station 47-C in the deeper canyon (at 1801 m WD) had the highest Chl *a* deposition rates ($0.4 \mu\text{g cm}^{-2} \text{y}^{-1}$) from all the stations. It was followed by station 54-S (at 343 m WD with $0.36 \mu\text{g cm}^{-2} \text{y}^{-1}$), station 50-C (at 1215 m WD with $0.3 \mu\text{g cm}^{-2} \text{y}^{-1}$) and station 51-S (at 1209 m WD with $0.13 \mu\text{g cm}^{-2} \text{y}^{-1}$); stations 48-C (at 2112 m WD with $0.007 \mu\text{g cm}^{-2} \text{y}^{-1}$) and 49-S (at 1874 m WD with $0.004 \mu\text{g cm}^{-2} \text{y}^{-1}$) had the lowest deposition rates. While Chl *a* deposition decreased with water depth on the slope, inside the canyon it was rather heterogeneous. The higher deposition rates at stations 50-C and 47-C seem to indicate that it is towards the middle canyon where sediment deposition is largest. Their results are supported by our observations on particle sorting, with high abundances of sand in this area but not further down-canyon. This suggests that an important part of sediment load of the DSWC is deposited around the middle canyon while the flow reaches its neutral buoyancy level (Canals et al., 2006; Sánchez-Vidal et al., 2009). Most likely, towards the upper canyon sedimentation is limited by the erosive action of the flow, while towards the distal lower canyon, located beyond the reach of DSWC, hemipelagic deposition prevails.

In the same study, García et al. (2008) modeled the decay rate and mixing intensities for chlorophyll *a* in the Cap de Creus canyon and adjacent slope area. The decay of Chl *a* had an exponential behavior on the upper few centimeters of sediment both in canyon and slope stations. Interestingly, biodiffusion coefficients were very similar for all the canyon stations ($0.09 \text{ cm}^2 \text{y}^{-1}$ for station 50-C and $0.12 \text{ cm}^2 \text{y}^{-1}$ for station 47-C and 48-C), while for the slope stations they decreased with water depth ($1.83 \text{ cm}^2 \text{y}^{-1}$ for station 54-S, $0.5 \text{ cm}^2 \text{y}^{-1}$ for station 51-S and $0.03 \text{ cm}^2 \text{y}^{-1}$ for station 49-S). This would be evidence of high bioturbation activity inside the canyon at all depths; which is supported by our observations on the ALD of benthic foraminiferal communities (Table 4). However, ALD of slope communities did not decrease with increasing water depth contrary to the suggested by biodiffusion coefficients.

The DCA plots (Fig. 10) provide a general characterization of the benthic environments from the Cap de Creus canyon and adjacent slope area, with all the geochemical parameters from this study taken into consideration. DCA axis 1 appears to reflect food quality, since the proportion of chlorophyll *a* with respect to the phaeopigments (and therefore the food freshness) decreased with increasing water depth. DCA axis 2 appears to reflect the environmental difference between canyon and slope settings in terms of food quantity, represented by the CPE vector which directs towards canyon environments. Therefore, in Fig. 10, the top left quadrant would represent environments with high quantity and high quality food, the top right quadrant would correspond to environments with intermediate to high quantity but low quality food, the bottom left quadrant would constitute environments with intermediate to low quantity but high quality food, and the bottom right quadrant would stand for environments with low quantity and low quality food.

According to the results, shallow stations (52-C and 54-S) show clear canyon or slope trends, which could result from the high particulate matter input that the canyon head receives due to DSWC. Stations in the deepest areas (47-C, 49-S and 38-C), however, show less differentiated conditions between canyon and slope characteristics. This could be explained by the reduced influence of DSWC and a more important influence of BNL and hemipelagic deposition which affect canyon and slope evenly (García et al., 2008; Tesi et al., 2010). These deep stations mostly respond to water depth and distance to the shore, as the main controllers of the food quality in these environments. Stations at intermediate depths (50-C and 51-S) are located in the quadrant of intermediate to high food quantity and intermediate to low food quality. The higher food quantity and quality of station 50-C could be reflecting the influence of DSWC in this area of the canyon even if it is very limited due its depth.

5.2 The dynamics between food supply, physical disturbance and benthic foraminiferal community structure

Benthic foraminiferal faunas within the canyon are well developed, as suggested by high diversity, higher evenness than slope stations at comparable water depths, deeper ALD, and the presence of infaunal species (Table 4 and Fig. 9B). This would be an indication of 'complex' communities contrary to what would be expected from the physical disturbance associated to the seasonal DSWC events. However, it is also important to take into account that the degree of physical disturbance is highly variable (intra- and inter-annual variation), and decreases towards deeper areas of the canyon; besides, major DSWC events are rare (Canals et al., 2006). On the basis of the sediment composition it is possible to say that the canyon head and the upper canyon sections are the most affected by physical disturbance derived from DSWC. Sediment sorting in these areas affected by currents activity results in higher proportion of sand and silt particles, and the eventual presence of shell fragments in the canyon head. Although this may suggest enhanced physical disturbance, the sampling stations (52-C and 50-C) are located towards the northern wall of the canyon where sediment accumulation is larger than erosion (de Geest et al., 2008). This may decrease the impact of physical disturbance on benthic foraminiferal communities.

For benthic foraminiferal communities of this area, the main difference between canyon and slope environments seems to be more related to the food availability and the associated in-sediment redox conditions (as indicated by the DCA analysis) than to the physical disturbance. Our results suggest that canyon environments can sustain more diverse communities with a more stable species composition in comparison to the slope, and therefore this should be linked to the differences in available food. In the Lacaze-Duthiers canyon (immediately to the north of the Cap de Creus canyon), Schmiedl et al. (2000) also observed that canyon benthic foraminiferal faunas were better developed than slope faunas at comparable water depth. Furthermore, they studied seasonal differences in faunal composition between canyon and slope and they found that canyon faunas were also stable throughout the year,

in contrast with slope faunas, which presented lower abundances and diversity during winter. Therefore, open slope environments seem more suitable to be dominated by opportunistic species, supporting the idea of more stable communities in the canyon at least in intermediate time scales. Unfortunately, the analysis of Schmiedl et al. (2000) was only performed for the upper canyon section, which gives an incomplete picture of the faunal dynamics within the whole canyon system.

5.3 Benthic foraminiferal assemblages from different trophic regimes

The Mediterranean Sea is generally regarded as oligotrophic compared to other oceans. Besides, Mediterranean waters are about 10°C warmer than deep waters in other oceans (de Rijk et al., 2000), which accelerates the degradation of organic matter in the water column. However, even in the Mediterranean some regions are more productive than others, and organic matter flux does generally decline with increasing water depth (de Rijk et al., 2000). Therefore, in this study we will describe and divide the benthic environments into three categories on the basis of the available geochemical and pigment data (Fig. 9A). Eutrophic environments will be regarded as those where sediment surface CPE concentrations were higher than 10 $\mu\text{g cm}^{-3}$ and NPD <1cm. In the case of this study, only the canyon head enters into this category, but most likely surface CPE concentrations of this order or higher occur more widely along the continental shelf. Environments with surface CPE concentrations between 3-10 $\mu\text{g cm}^{-3}$ and NPD between 2-7 cm will be regarded here as mesotrophic benthic environment. These comprise all the shallow and intermediate slope area, the upper and middle canyon sections, and the proximal lower canyon area. Finally, oligotrophic benthic environments will be regarded as those with surface CPE concentrations lower than 3 $\mu\text{g cm}^{-3}$ and NPD >7 cm. These include the deep slope area and the most distal lower canyon section.

5.3.1 Benthic foraminifera from eutrophic environments

Eutrophic environments were dominated by species of *A. pseudospiralis* and *C. ungerianus* regarded as shallow to intermediate infaunal species. According to their distribution in the TROX map, *A. pseudospiralis* and *C. ungerianus* occur where surface CPE concentrations >10 $\mu\text{g cm}^{-3}$ and their in-sediment distribution tracks the CPE >3 $\mu\text{g cm}^{-3}$ isoline without restrictions related to the sediment redox conditions. However, *A. pseudospiralis* has higher abundances deeper in the sediment (over 30 individuals at 4 cm depth), while *C. ungerianus* displays a surface maximum. In the DCA plots, *C. ungerianus* is located in the area of high food quality and abundance, being the species with the strictest requirements in this matter of all the species included in the analysis. Both species have been associated with environments with high food supply and oxygen depletion (Alve and Nagy, 1986); (Jorissen et al., 2007). Other common species in these environments is *S. sagittula*, which displayed shallow to intermediate

infaunal distribution (Fig 9B), similar to the two previously mentioned species. In the DCA plot, it is located very close to *C. ungerianus* indicating it high quality food preferences. *S. sagittula* species has been reported as a common shelf species in the Mediterranean associated to sandy substrates and also to energetic environments (de Stigter et al., 1998; Milker et al., 2009; Schönfeld, 2002).

In the 63-150 μm fraction, common species are *B. spathulata* and *C. laevigata* which, in the DCA plots, are located in the region of high food quality and intermediate to high food abundance. Both of them are commonly associated with areas of high organic matter input and dysoxic to anoxic conditions occupying (Chendes et al., 2004; Debanay and Redois, 1997; Jorissen et al., 2007; Licari and Mackensen, 2005; Milker et al., 2009; Mojtahid et al., 2009; Schumacher et al., 2007).

5.3.1 Benthic foraminifera from mesotrophic environments

Mesotrophic environments of shallow to intermediate-deep areas (<1200 m WD) were dominated by the species *U. mediterranea* and *B. nodosaria*, present in, both, canyon and slope. The species *U. mediterranea* is a shallow infaunal taxa with highest abundances in well-oxygenated areas in environments under relatively high phytodetritus input (CPE >2.6 $\mu\text{g cm}^{-3}$ in the surface and >1 $\mu\text{g cm}^{-3}$ within the sediment). These results are in agreement with the observations made by other authors (Fontanier et al., 2008; Geslin et al., 2004; Jorissen et al., 2007; Koho et al., 2008; Schmiedl et al., 2000). The species *B. nodosaria* is an intermediate infaunal taxa with the highest abundances towards the surface and a second subsurface maximum around 2-3 cm sediment depth. Its in-sediment distribution seems to track the >2 $\mu\text{g cm}^{-3}$ isoline (not shown). The DCA plots indicate its preference for high food quality although in intermediate quantities. It has previously been associated with muddy sand substrates and able to tolerate dysoxic conditions (Chendes et al., 2004; Murray, 2006).

The species *B. cylindrica*, *B. aculeata* and *T. agglutinans* were also common in shallow to intermediate-deep (<1200 m WD) mesotrophic environments. In our DCA analysis, *B. cylindrica*, *B. aculeata* and *T. agglutinans* seem to prefer high quality food in intermediate quantities. These species have been frequently associated with shallow to intermediate infaunal microhabitats under meso-eutrophic conditions in marine environments with continental influence (Fontanier et al., 2008; Koho et al., 2008; Koho et al., 2007; Mojtahid et al., 2009; Oliveira-Silva et al., 2005).

At intermediate water depths (~1200 m WD) other species become more important in mesotrophic environments, like *C. cf. mamilla*, *M. barleeanus*. The species *C. cf. mamilla* is present only inside the canyon. According to the DCA plots, this species prefers canyon environments where food is still relatively abundant (surface CPE concentrations >2.6 $\mu\text{g cm}^{-3}$) but of intermediate quality (Chl *a*/Phaeo ~0.02). *C. mamilla* has been previously reported as an

epibenthic to shallow infaunal species, with deposit feeding habits on detrital material and associated to high energy environments where it profits from currents activity (Gooday et al., 1996; Schönfeld, 2002). Its absence on slope environments of equivalent depth, where the food quality is similar, could be explained by the weaker current activity. On the other hand, the canyon is still under the influence of current activity, as indicated by the presence of mega-furrows on the canyon floor (Lastras et al., 2007). The intermediate to deep infaunal species *M. barleeanus* also becomes abundant in the distal reach of the upper canyon. The DCA analysis places *M. barleeanus* in the group of species associated with high quality but intermediate quantity food preferences (Chl *a*/Phaeo ratio ~0.02 and in-sediment CPE concentrations $>1 \mu\text{g cm}^{-3}$). This species has been reported to occur in oxic to dysoxic organic rich sediments although the quality of the organic matter can be variable (Fontanier et al., 2008; Jorissen et al., 2007; Koho et al., 2007; Licari and Mackensen, 2005). The limit of its vertical distribution seems to coincide with the redox front and the nitrate reduction zone (Fontanier et al., 2005; Fontanier et al., 2008; Koho et al., 2008). Koho et al. (2008) report maximum abundances of this species in sediments rich in labile phytodetritus which is in agreement with our observations.

In the 63-150 μm fraction, *E. pusillus* becomes important in terms of abundance at intermediate depths both in canyon and slope areas and remains a dominant component of the assemblages in deeper oligotrophic regions. In the DCA plots, this species appears towards the area of intermediate food quantities (surface CPE $<2.6 \mu\text{g cm}^{-3}$) and low quality (Chl *a*/Phaeo ratio <0.02). *E. pusillus* seems to display an opportunistic life style blooming right after the deposition of fresh phytodetritus in the deep ocean (Gooday and Hughes, 2002), which in the present study could be associated with the early spring bloom of phytoplankton observed by Fabres et al. (2008) between February and March of 2004.

5.3.1 Benthic foraminifera from oligotrophic environments

Oligotrophic environments were dominated by species such as the unidentified “agglutinated-dome”, *A. clavata* and *G. charoides* in the $>150 \mu\text{m}$ fraction; whereas *E. pusillus* maintained high abundances in the 63-150 μm fraction. With regard to the agglutinated-dome species, it dominated the assemblages in locations where most of other species were unsuccessful (surface CPE concentrations $<2 \mu\text{g cm}^{-3}$), suggesting a life style based on high efficiency in food exploitation. On the basis of its wall morphology as well as its living position the agglutinated-dome could be related to the genus *Sorosphaera* (A. Gooday, personal communication, 2010).

The species *A. clavata* was abundant in the proximal part of the lower canyon while *G. charoides* was it in the most distal part. However, *G. charoides* was also found all the way towards the mesotrophic middle canyon, where it reached high abundances. Both species appear in the area of low quality food exploitation in the DCA analysis plot. The high abundances of *G. charoides* in mesotrophic environments suggest affinity to more labile organic matter in

the sediments; nevertheless, it only seems to become dominant in areas where food amounts become too low for other species (surface CPE $<2 \mu\text{g cm}^{-3}$). The species, *A. clavata* has a more specialized habitat, occurring only in the canyon and only in the top centimeter of sediment (CPE $\sim 2.45 \mu\text{g cm}^{-3}$ and Chl *a*/Phaeo = 0.01), maybe profiting from the surface currents. This species has previously been observed in oligotrophic environments (Nigam et al., 2004) and with sediments with low quality organic matter (low lipids concentration; (Fontanier et al., 2008).

5.4 Arborescent and tubular agglutinated foraminifera in the Cap de Creus canyon and slope areas

This group of foraminifera was present in almost all the analyzed samples from the Cap de Creus canyon and adjacent slope. The middle canyon, station 50-C, showed the highest abundances of arborescent and tubular benthic foraminifera fragments, indicating that in this environment they can reach large sizes. Most likely, at this site a good balance exists between the benefits of bottom current activity (sampled station is located on the canyon's thalweg) and a moderate energy level.

Saccorhiza ramosa is one of the most abundant arborescent foraminifera within the canyon in mesotrophic environments (surface CPE $\sim 3 \mu\text{g cm}^{-3}$); however, this species is also present in the distal reach of the Cap de Creus canyon and its adjacent slope under oligotrophic conditions (surface CPE $<3 \mu\text{g cm}^{-3}$). It presented clear peak abundances between the sediment surface and 1.5 cm within the sediment column in stations 50-C and 51-S, with a deeper habitat in the canyon than on the slope. Fragments were still observed down to 2 cm within the sediment. This species seems to prefer an elevated position above the sediment-water interface to catch suspended food particles transported by the bottom currents and is common in the area of the Gulf of Lions, both in canyon and slope environments (Schmiedl et al., 2000). Koho et al. (2008) and Koho et al. (2007) report the occurrence of this species in the Lisbon-Setúbal and Nazaré canyons respectively, living in the deepest areas at the distal end of the canyons, usually under oligotrophic conditions (surface CPE concentrations $<2 \mu\text{g cm}^{-3}$) and low current speeds. Schröder-Adams et al. (2008) also associate this species with turbidity currents and suspended sediment supply but in semi-sheltered habitats. Another very abundant species was *Dendrophrya* sp., which occurred in mesotrophic environments with highest abundances in the upper canyon section. It had peak abundances in the top 0.5 cm within the sediment, but fragments were still found down to 1.5 cm. This genus has previously been observed as a common epifauna, most probably feeding on suspended particles (Kaminski et al., 1988). Its high abundance in at station 50-C in the upper canyon thalweg points to a stable population that profits from the organic matter transported by the cascading water.

The species *Rhabdammina linearis* occurred in mesotrophic stations of intermediate depth (50-C and 51-S) but it is more abundant in the canyon than on the slope, suggesting that its lifestyle is favored by the action of local bottom currents. Its vertical distribution in our samples goes down to 2 cm but did not show peak abundances at any particular depth. This species is also classified as an epifaunal species with suspension feeding habits in mesotrophic and deep-sea environments (Gooday, 1983; Gooday et al., 2001a; Gooday et al., 2001b). Species of the genus *Hyperammina* were found mostly in eutrophic/ mesotrophic environments, with the exception of *H. elongata* which was mostly confined to mesotrophic /oligotrophic areas. Most of the species were living in the topmost part of the sediment column, whereas *H. elongata* presented its maximum abundances between 0.5 and 1 cm within the sediment in station 51-S. Species of the genus *Hyperammina* have been catalogued as detritivores, and likely to colonize deep-sea environments with seasonal phytodetritus deposition (Murray, 2006). Four species of the genus *Bathysiphon* occurred in the stations regarded as meso-eutrophic (52-C, 54-S, 50-C and 51-S); however three out of four were not found at station 52-C, possibly due to the stronger energetic regime of the canyon head. *Bathysiphon* species have been found in submarine canyons where their abundance seems to be related with medium to high organic carbon input and relatively low oxygen penetration depth (Koho et al., 2008; Koho et al., 2007). The absence of most of these species at the canyon head is supported by the observations of Koho et al. (2008) who reported the occurrence of these species in the Nazaré canyon terraces but not in the strongly disturbed canyon axis.

5.5 Cap de Creus canyon benthic foraminifera in comparison to other canyon systems

The relationship between living benthic foraminifera communities, food abundance and habitat instability in canyon ecosystems has been previously studied by Koho et al. (2007) and Koho et al. (2008) in the Nazaré and Lisbon-Setúbal canyons respectively. These two canyon systems have some particular characteristics that make them considerably different from the Cap de Creus canyon. For instance, the Nazaré and Lisbon-Setúbal canyons are long (220 km and 180 km), deeply incised (2-2.5 km and 1.5-2 km) narrow (>100 m and ~100 m thalweg width) canyons, in which the sediment transport is driven by the action of tidal currents, gravity flows and turbidity currents (Arzola et al., 2008; de Stigter et al., 2007). Both canyons are located under an area of high surface productivity (154 to 556 g C m⁻² y⁻¹) (Álvarez-Salgado et al., 2003). In contrast, the Cap de Creus canyon is a relatively short (96 km), shallowly incised (500-700 m) wide (~600 m thalweg width) canyon, in which the sediment transport is driven by dense shelf water downwelling and cascading. Besides, the Cap de Creus canyon is located under an area of relatively low surface productivity (78 to 142 g C m⁻² y⁻¹) (Lefevre et al., 1997) and has a larger continental shelf.

These features have important consequences for the benthic foraminiferal faunas in several aspects. The first one of them is associated to the energetic regime. While high benthic foraminifera TSS have been found in the upper canyon axis of the Cap de Creus (CdC) canyon (59-232 individuals per 50 cc) and the Lisbon-Setúbal (L-S) canyon (57-270 individuals per 50 cc) (Koho et al., 2008), this is not the case for the Nazaré canyon axis, in which the intense physical disturbance seems to impede the development of well-established benthic communities. High TSS (183-316 individuals per 50 cc) were found, however, living in lateral terraces in the upper canyon section, where they would still profit from high labile organic matter inputs but in a low-disturbed environment (Koho et al., 2007). Comparing our geochemical measurements with those of Koho et al. (2007, 2008) we observe that sediment surface CPE concentrations during spring (May) were similar in the three most upper section of the canyons, $17.8 \mu\text{g cm}^{-3}$, $21.71 \mu\text{g cm}^{-3}$ and $15.15 \mu\text{g cm}^{-3}$ for the CdC, L-S and Nazaré around 300 m WD. However, sediment surface CPE values decrease radically with water depth in the CdC canyon ($2.45 \mu\text{g cm}^{-3}$ at 1801 m WD) whereas they remain high for the L-S ($8.56 \mu\text{g cm}^{-3}$ at 1855 m WD) and the Nazaré ($18.48 - 9.72 \mu\text{g cm}^{-3}$ at 1118 and 2847 m WD respectively) canyons. The higher CPE values in the Portuguese margin canyons can be associated to the higher primary production at surface waters, especially during spring months. Chl *a*/Phaeo ratios around 300 m WD are 0.09, 0.044 and 0.048 for Nazaré, L-S and CdC respectively; however they decrease to 0.019 (CdC 1801 m WD), 0.028 (L-S 1855 m WD) and 0.03 (Nazaré 2874 m WD). At 1118 m WD in the middle section of the Nazaré canyon, the Chl *a*/Phaeo ratio reached the record value of 0.18, the highest observed for any section of the three studied canyons, interestingly the observed TSS are lower than in other areas (19 individuals per 50 cc)(Koho et al., 2007).

Clearly, the Nazaré canyon axis presents higher food abundances and better food quality at similar and even greater depths than the other two canyons. However, TSS here are not determined by the fresh food abundance but by physical disturbance. In the case of the L-S and the CdC canyons, TSS are mostly determined by fresh food abundance and seem to be less affected by physical disturbance. Observations made in the adjacent slope of the L-S and CdC canyons also show that productivity is usually higher inside the canyon environments, while the difference between canyon and slope productivity decreases with increasing water depth. Inside the Lisbon-Setúbal canyon, sediment surface CPE concentrations ranged from $21.71 \mu\text{g cm}^{-3}$ at 365 m WD to $1.18 \mu\text{g cm}^{-3}$ at 4450 m WD, while they ranged from $16.09 \mu\text{g cm}^{-3}$ at 300 m WD to $1.95 \mu\text{g cm}^{-3}$ at 2945 m WD on the adjacent slope (Koho et al., 2008). Inside the Cap de Creus canyon, sediment surface CPE concentrations ranged from $15.15 \mu\text{g cm}^{-3}$ at 344 m WD to $1.45 \mu\text{g cm}^{-3}$ at 2112 m WD, whereas they ranged from $2.53 \mu\text{g cm}^{-3}$ at 343 m WD to $1.50 \mu\text{g cm}^{-3}$ at 1874 m WD on the adjacent slope. However, Chl *a*/Phaeo ratios were similar at similar water depths between canyon and slope environments in both canyons. Despite the differences in CPE concentrations, the similar distribution of Chl *a*/Phaeo ratios in both canyons suggests the existence of general common trends between submarine canyons even if they are affected by different processes.

Benthic foraminifera species composition can bring more light into these observations. Among the similarities between the two canyons, is the occurrence of meso-eutrophic species like *U. mediterranea* in environments with high surface CPE concentrations ($>10 \mu\text{g cm}^{-3}$ for the L-S canyon, and $>3 \mu\text{g cm}^{-3}$ for the CdC canyon, notice that the difference is 3 times higher in L-S canyon). In the L-S canyon, the species *M. barleeanus* was also associated with CPE rich sediments ($>4 \mu\text{g cm}^{-3}$) but its distribution was strongly influenced by the NO_3^- concentrations and it seemed to track denitrification front. In the CdC, it also occurred in environments with in-sediment CPE concentrations $>2 \mu\text{g cm}^{-3}$; however, the species did not track the redox front as closely although its distribution was usually limited to the upper part of the dysoxic area (NO_3^- concentrations $>4 \mu\text{mol L}^{-1}$).

It is worth to notice the low abundance of deep infaunal species of the genera *Globobulimina* and *Chilostomella* which are common in eutrophic environments with strong oxygen depletion (Jorissen et al., 2007; Jorissen et al., 1995; Koho et al., 2008; Koho et al., 2007). Although these species were found in the analyzed samples, they never occurred in high abundances. This is a good indication of the general low-nutrient character of the Gulf of Lions continental margin as compared to high productivity regions, for example the Portuguese margin (Álvarez-Salgado et al., 2003; García et al., 2008; García and Thomsen, 2008). In the sediments of the L-S canyon, these species occur when CPE concentrations are higher than $4 \mu\text{g cm}^{-3}$ down to 5 cm within the sediments (concentrations of more than $10 \mu\text{g cm}^{-3}$ occur at these depths in the most eutrophic stations) (Koho et al., 2008). In the CdC canyon, the only stations that present more than $3 \mu\text{g cm}^{-3}$ in the top 5 cm of sediment are 52-C, 54-S and 50-C and these are also the only stations where the species occur. However, these CPE concentrations seems to represent the lower limit of food requirements of these species, therefore, they are not highly abundant under these conditions.

Together with the low abundance of deep infaunal species, it is worth to notice the higher abundance of agglutinated species such as *A. pseudospiralis*, *B. nodosaria*, *B. cylindrical*, *S. sagittula* and *T. agglutinans* in the meso-eutrophic areas of the CdC canyon in comparison to the canyons at the Portuguese margin. The relative abundance of agglutinated species has been observed to increase in relation to calcareous species as a result of reduced fresh organic matter supply; this is because agglutinated foraminifera seem to have a varied diet and are able to profit from both fresh and degraded organic phytodetritus (Alve, 2010). The high abundance of agglutinated foraminifera in meso-eutrophic environments of the CdC canyon could be a response to the heterogeneous conditions of the canyon. This is because the availability of fresh phytodetritus may vary depending on the strength and timing of the DSWC, i.e. if it was produced before or after the early spring phytoplankton blooms and how far does the phytodetritus plume travels down-canyon. In this way, agglutinated species would profit from any kind of organic matter carried by the DSWC, in contrast with calcareous species which rely more on the availability of fresh phytodetritus (Alve, 2010).

With respect to the agglutinated, tubular and arborescent benthic foraminifera, in the Nazaré canyon species of the genus *Technitella*, *Chrithionina* and *Bathysiphon* are usually abundant in eutrophic environments with surface CPE concentrations $>18 \mu\text{g cm}^{-3}$, whereas *Saccorhiza ramosa* was found in deeper more oligotrophic environments with surface CPE concentrations $<2 \mu\text{g cm}^{-3}$ (Koho et al., 2008). In particular, *Technitella* was associated with physically disturbed environments. In the CdC canyon, species of *Technitella*, *Chrithionina* and *Bathysiphon* are found in mesotrophic environments, where surface CPE concentrations are much lower ($>3 \mu\text{g cm}^{-3}$). Species of *Technitella* and *Chrithionina* were also associated with physically disturbed environments. *Saccorhiza ramosa* was also found in oligotrophic environments of the CdC canyon, but had highest abundances (fragments) in mesotrophic conditions (surface CPE $\sim 3 \mu\text{g cm}^{-3}$). Species from the genus of *Reophax* and *Lagenammia* which are conferred to oligotrophic environments in the Nazaré canyon (surface CPE = $1-3 \mu\text{g cm}^{-3}$) are found mostly in meso-eutrophic environments in the CdC canyon whose surface CPE concentrations are higher than $3 \mu\text{g cm}^{-3}$, which is the upper boundary of oligotrophic conditions for the Nazaré canyon.

6. Conclusions

- Chl *a*/Phaeo ratio (food quality) and CPE concentrations (food quantity) seemed to be more important than bulk organic carbon in determining the food availability for benthic foraminiferal communities, and they also play a key role shaping their abundance and ecosystem or assemblage structure.
- The decrease of food quality (Chl *a*/Phaeo ratio) with water depth represents the most important factor determining the distribution of benthic foraminifera both in canyon and slope environments, whereas the increase of food quantity (CPE concentrations) from slope to canyon environments represents the second most important factor.
- Shallow stations (<400 m WD) had well separated canyon or slope characteristics in terms of food quantity and quality; however, the difference becomes considerably smaller towards deeper (>1500 m WD) stations. This could be indicating that the influence of DSWC events is limited to the canyon head and the upper canyon sections.
- Eutrophic environments only occurred at the canyon head where communities were dominated by the species *A. pseudospiralis* and *C. ungerianus* in the $>150 \mu\text{m}$ fraction, and *B. spathulata* and *C. laevigata* in the $63-150 \mu\text{m}$ fraction. The lack of deep infaunal taxa such as *Globobulimina* spp. and *Chilostomella* spp. denotes that these environments are in the lower boundary of eutrophic conditions and point out the general oligotrophic nature of the Gulf of Lions in comparison to other ocean basins.
- Mesotrophic environments were found in the shallow open slope and at intermediate depths both in canyon and slope environments. The most abundant species were *Uvigerina mediterranea* and *Bigenerina*

nodosaria in the >150 μm fraction, and *Bolivina spathulata* and *Eponides pusillus* in the 63-150 μm fraction. Inside the canyon the species *Crithionina cf. mamilla* high abundance in the assemblages, giving evidence of current activity at least to some extent. Fragments from arborescent and tubular species were also abundant in this kind of environments. In particular, the species *Saccorhiza ramosa* and *Dendrophrya* sp. had very high fragments abundance in the upper canyon area.

- Oligotrophic environments occurred in the deepest canyon and slope areas and communities were dominated by *Ammolagena clavata*, *Glomospira charoides* and an unidentified single-chambered “agglutinated dome” species in the >150 μm fraction, and by *G. charoides* and *E. pusillus* in the 63-150 μm fraction. Most likely, *E. pusillus* has an opportunistic life style and seems to profit from the rain of fresh organic matter produced during the spring phytoplankton blooms.
- The high abundance of agglutinated species in the meso-eutrophic canyon environments may indicate the variable character of the organic matter advected by DSWC, which would depend on the timing and strength of the events. Agglutinated taxa seem to be able to profit from more varied kinds of phytodetritus, fresh or degraded, compared to calcareous taxa, which depend mostly on the fresh one.

7. References

- Álvarez-Salgado, X.A., Figueiras, F.G., Pérez, F.F., Groom, S., Nogueira, E., Borges, A.V., Chou, L., Castro, C.G., Moncoiffé, G., Ríos, A.F., Miller, A.E.J., Frankignoulle, M., Savidge, G., and Wollast, R., 2003, The Portugal coastal counter current off NW Spain: new insights in its biogeochemical variability: *Progress in Oceanography*, v. 56, p. 281-321.
- Alve, E., 2010, Benthic foraminiferal responses to absence of fresh phytodetritus: A two-year experiment: *Marine Micropaleontology*, v. doi:10.1016/j.marmicro.2010.05.003, p. (in press).
- Alve, E., and Nagy, J., 1986, Estuarine foraminiferal distribution in Sandebukta, a branch of the Oslo Fjord: *Journal of Foraminiferal Research*, v. 16, p. 261-284.
- Arzola, R.G., Wynn, R.B., Lastras, G., Masson, D.G., and Weaver, P.P.E., 2008, Sedimentary features and processes in the Nazaré and Setúbal submarine canyons, west Iberian margin: *Marine Geology*, v. 250, p. 64-88.
- Bourrin, F., Madron, X.D.d., Heussener, S., and Estournel, C., 2008, Impact of winter dense water formation on shelf sediment erosion (evidence from the Gulf of Lions, NW Mediterranean): *Continental Shelf Research*, v. 28, p. 1984-1999.
- Canals, M., Puig, P., Madron, X.D.d., Heussner, S., Palanques, A., and Fabres, J., 2006, Flushing submarine canyons: *Nature*, v. 444, p. 354-357.
- Chendes, C., Kaminski, M.A., Filipescu, S., Aksu, A.E., and Yasar, D., 2004, The response of modern benthic foraminiferal assemblages to water-mass properties along the southern shelf of the Marmara Sea: *Acta Paleontologica Romaniaae*, v. 4, p. 69-80.
- Debanay, J.P., and Redois, F., 1997, Recent foraminifera of the northern continental shelf of Senegal: *Revue de Micropaléontologie*, v. 40, p. 15-38.

- de Geest, A.L., Mullenbach, B.L., Puig, P., Nittrouer, C.A., Drexler, T.M., Madron, X.D.d., and Orange, D.L., 2008, Sediment accumulation in the western Gulf of Lions, France: The role of Cap de Creus Canyon in linking shelf and slope sediment dispersal systems: *Continental Shelf Research*, v. 28, p. 2031-2047.
- de Rijk, S., Jorissen, F.J., Rohling, E.J., and Troelstra, S.R., 2000, Organic flux control on bathymetric zonation of Mediterranean benthic foraminifera: *Marine Micropaleontology*, v. 40, p. 151-166.
- de Stigter, H.C., Boer, W., Mendes, P.A.d.J., Jesus, C.C., Thomsen, L., Bergh, G.D.v.d., and Weering, T.C.E.v., 2007, Recent sediment transport and deposition in the Nazaré Canyon, Portuguese continental margin: *Marine Geology*, v. 246, p. 144-164.
- de Stigter, H.C., Jorissen, F.J., and Zwaan, G.J.v.d., 1998, Bathymetric distribution and microhabitat partitioning of live (Rose Bengal stained) benthic foraminifera along a shelf to deep sea transect in the southern Adriatic Sea: *Marine Micropaleontology*, v. 28, p. 40-65.
- Fabres, J., Tesi, T., Velez, J., Batista, F., Lee, C., Calafat, A., Heussner, S., Palanques, A., and Miserocchi, S., 2008, Seasonal and event-controlled export of organic matter from the shelf towards the Gulf of Lions continental slope: *Continental Shelf Research*, v. 28, p. 1971-1983.
- Fontanier, C., Jorissen, F.J., Chaillou, G., Anschutz, P., Grémare, A., and Griveaud, C., 2005, Live foraminiferal faunas from a 2800 m deep lower canyon station from the Bay of Biscay: Faunal response to focusing of refractory organic matter: *Deep-Sea Research I*, v. 52, p. 1189-1227.
- Fontanier, C., Jorissen, F.J., Lansard, B., Mouret, A., Buscail, R., Schmidt, S., Kerhervé, P., Buron, F., Zaragosi, S., Hunault, G., Ernoult, E., Artero, C., Anschutz, P., and Rabouille, C., 2008, Live foraminifera from the open slope between Grand Rhône and Petit Rhône Canyons (Gulf of Lions, NW Mediterranean): *Deep-Sea Research I*, v. 55, p. 1532-1553.
- García, R., Oevelen, D.v., Soetaert, K., Thomsen, L., Stigter, H.C.D., and Epping, E., 2008, Deposition rates and mixing intensity and organic content in two contrasting submarine canyons: *Progress in Oceanography*, v. 76, p. 192-215.
- García, R., and Thomsen, L., 2008, Bioavailable organic matter in surface sediments of the Nazaré canyon and adjacent slope (Western Iberian Margin): *Journal of Marine Systems*, v. 74, p. 44-59.
- Geslin, E., Heinz, P., Jorissen, F., and Hemleben, C., 2004, Migratory responses of deep-sea benthic foraminifera to variable oxygen conditions: laboratory investigations: *Marine Micropaleontology*, v. 53, p. 227-243.
- Gooday, A.J., 1983, Primitive Foraminifera and Xenophyphorea in IOS epibenthic sledge samples from the northeast Atlantic, Volume 156, Institute of Oceanographic Sciences, p. 33.
- , 1988, A response by benthic Foraminifera to the deposition of phytodetritus in the deep sea: *Nature*, v. 332, p. 70-73.
- Gooday, A.J., Bowser, S.S., and Bernhard, J.M., 1996, Benthic foraminiferal assemblages in Explorers Cove, Antarctica: A shallow-water site with deep-sea characteristics: *Progress in Oceanography*, v. 37, p. 117-166.
- Gooday, A.J., Hughes, A.J., and Levin, L.A., 2001a, The foraminiferan macrofauna from three North Carolina (USA) slope sites with contrasting carbon flux: a comparison with the metazoan macrofauna: *Deep-Sea Research I*, v. 48, p. 1709-1739.
- Gooday, A.J., and Hughes, J.A., 2002, Foraminifera associated with phytodetritus deposits at a bathyal site in the northern Rockall Trough (NE Atlantic): seasonal contrasts and a comparison of stained and dead assemblages: *Marine Micropaleontology*, v. 46, p. 83-110.
- Gooday, A.J., Kitazato, H., Hori, S., and Toyofuku, T., 2001b, Monothalamous soft-shelled Foraminifera at an abyssal site in the North Pacific: A preliminary report: *Journal of Oceanography*, v. 57, p. 377-384.
- Gooday, A.J., Levin, L.A., Linke, P., and Heeger, T., 1992, The role of benthic foraminifera in deep-sea food webs and carbon cycling, *in* Rowe, G.T., and Patience, V., eds., *Deep-sea food chains and the global carbon cycle: The Netherlands*, Kluwer Academic Publishers, p. 63-91.

- Grashoff, K., Erhardt, M., and Kremling, K., 1983, *Methods of seawater analysis*: Weinheim, Germany, Verlag Chemie, 419 p.
- Hedges, J.I., Keil, R.G., and Benner, R., 1997, What happens to terrestrial organic matter in the ocean?: *Organic Geochemistry*, v. 27, p. 195-212.
- Helder, W., 1989, Early diagenesis and sediment-water exchange in the Savu Basin (Eastern Indonesia): *Netherlands Journal of Sea Research*, v. 24, p. 555-572.
- Heussener, S., Madron, X.D.d., Calafat, A., Canals, M., Carbonne, J., Desaut, N., and Saragoni, G., 2006, Spatial and temporal variability of downward particle fluxes on a continental slope: Lessons from an 8-yr experiment in the Gulf of Lions (NW Mediterranean): *Marine Geology*, v. 234, p. 63-92.
- Jensen, K., Sloth, N.P., Risgaard-Petersen, N., Rysgaard, S., and Revsbech, N.P., 1994, Estimation of nitrification and denitrification from microprofiles of oxygen and nitrate in model sediment systems: *Applied and environmental microbiology*, v. 60, p. 2094-2100.
- Jorissen, F.J., Fontanier, C., and Thomas, E., 2007, Paleooceanographical proxies based on deep-sea benthic foraminiferal assemblage characteristics, *Developments in Marine Geology, Volume 1*, Elsevier B.V., p. 277-340.
- Jorissen, F.J., Stigter, H.C.d., and Widmark, J.G.V., 1995, A conceptual model explaining benthic foraminiferal microhabitats: *Marine Micropaleontology*, v. 26, p. 3-15.
- Kaminski, M.A., Grassle, J.F., and Whitlatch, R.B., 1988, Life history and recolonization among agglutinated foraminifera in the Panama Basin: *Abh. Geol. B.-A.*, v. 41, p. 229-243.
- Koho, K.A., García, R., Stigter, H.C.d., Epping, E., Koning, E., Kouwenhoven, T.J., and Zwaan, G.J.v.d., 2008, Sedimentary labile organic carbon and pore water redox control on species distribution of benthic foraminifera: A case study from Lisbon-Setúbal Canyon (southern Portugal): *Progress in Oceanography*, v. 79, p. 55-82.
- Koho, K.A., Kouwenhoven, T.J., Stigter, H.C.d., and Zwaan, G.J.v.d., 2007, Benthic foraminifera in the Nazaré Canyon, Portuguese continental margin: Sedimentary environments and disturbance: *Marine Micropaleontology*, v. 66, p. 27-51.
- Lastras, G., Canals, M., Urgeles, R., Amblas, D., Ivanov, M., Droz, L., Dennielou, B., Fabrès, J., Schoolmeester, T., Akhmetzhanov, A., Orange, D., and García-García, A., 2007, A walk down the Cap de Creus canyon, Northwestern Mediterranean Sea: Recent process inferred from morphology and sediment bedforms: *Marine Geology*, v. 246, p. 176-192.
- Lefevre, D., Minas, H.J., Minas, M., Robinson, C., Williams, P.J.L.B., and Woodward, E.M.S., 1997, Review of gross community production, primary production, net community production and dark community respiration in the Gulf of Lions: *Deep-Sea Research II*, v. 44, p. 801-832.
- Licari, L., and Mackensen, A., 2005, Benthic foraminifera off West Africa: Do live assemblages from the topmost sediment reliably record environmental variability?: *Marine Micropaleontology*, v. 55.
- Lohse, L., Kloosterhuis, R.T., Stigter, H.C.d., Helder, W., Raaphorst, W.v., and Weering, T.C.E.v., 2000, Carbonate removal by acidification causes loss of nitrogenous compounds in continental margin sediments: *Marine Chemistry*, v. 69, p. 193-201.
- Milker, Y., Schmiedl, G., Betzler, C., Römer, M., Jaramillo-Vogel, D., and Siccha, M., 2009, Distribution of recent benthic foraminifera in shelf carbonate environments of the Western Mediterranean Sea: *Marine Micropaleontology*, v. 73, p. 207-225.
- Mojtahid, M., Jorissen, F., Lansard, B., Fontanier, C., Bombled, B., and Rabouille, C., 2009, Spatial distribution of live benthic foraminifera in the Rhône prodelta: Faunal response to continental-marine organic matter gradient: *Marine Micropaleontology*, v. 70, p. 177-200.
- Murray, J.W., 2006, *Ecology and applications of benthic foraminifera*, Cambridge University Press.

- Nigam, R., Mazumder, A., and Saraswat, R., 2004, *Ammolagena clavata* (Jones and Parker, 1860), an agglutinated benthic foraminiferal species - first report from the recent sediments, Arabain Sea, Indian Ocean region: *The Journal of Foraminiferal Research*, v. 34, p. 74-78.
- Oliveira-Silva, P., Fernandes-Barbosa, C., and Soares-Gomes, A., 2005, Distribution of macrobenthic foraminifera on Brazilian continental margin between 18°S - 23°S: *Revista Brasileira de Geociências*, v. 35, p. 209-216.
- Palanques, A., Guillén, J., Puig, P., and Madron, X.D.d., 2008, Storm-driven shelf-to-canyon suspended sediment transport at the southwestern Gulf of Lions: *Continental Shelf Research*, v. 28, p. 1947-1956.
- Palanques, A., Madron, X.D.d., Puig, P., Fabres, J., Guillén, J., Calafat, A., Canals, M., Heussner, S., and Bonnin, J., 2006, Suspended sediment fluxes and transport processes in the Gulf of Lions submarine canyons. The role of storms and dense water cascading: *Marine Geology*, v. 234, p. 43-61.
- Sánchez-Vidal, A., Pasqual, C., Kerhervé, P., Heussner, S., Calafat, A., Palanques, A., Madron, X.D.d., Canals, M., and Puig, P., 2009, Across margin export of organic matter by cascading events traced by stable isotopes, northwestern Mediterranean Sea: *Limnology and Oceanography*, v. 54, p. 1488-1500.
- Schmiedl, G., Bovée, F.d., Buscail, R., Charrière, B., Hemleben, C., Medernach, L., and Picon, P., 2000, Trophic control of benthic foraminiferal abundance and microhabitat in the bathyal Gulf of Lions, western Mediterranean Sea: *Marine Micropaleontology*, v. 40, p. 167-188.
- Schönfeld, J., 2002, A new benthic foraminiferal proxy for near-bottom current velocities in the Gulf of Cadiz, northeastern Atlantic Ocean: *Deep-Sea Research I*, v. 49, p. 1853-1875.
- Schumacher, S., Jorissen, F.J., Dissard, D., Larkin, K.E., and Gooday, A.J., 2007, Live (Rose Bengal stained) and dead benthic foraminifera from the oxygen minimum zone of the Pakistan continental margin (Arabian Sea): *Marine Micropaleontology*, v. 62, p. 45-73.
- Shröder-Adams, C.J., Boyd, R., Ruming, K., and Sandstrom, M., 2008, Influence of sediment transport dynamics and ocean floor morphology on benthic foraminifera, offshore Fraser Island, Australia: *Marine Geology*, v. 254, p. 47-61.
- Tesi, T., Miserocchi, S., Goñi, M.A., and Langone, L., 2007, Source, transport and fate of terrestrial organic carbon on the western Mediterranean Sea, Gulf of Lions, France: *Marine Chemistry*, v. 105, p. 101-117.
- Tesi, T., Puig, P., Palanques, A., and Goñi, M.A., 2010, Lateral advection of organic matter in cascading-dominated submarine canyons: *Progress in Oceanography*, v. 84, p. 185-203.
- Thiel, H., 1978, Benthos in upwelling regions, *in* Boje, R., and Tomczak, M., eds., *Upwelling ecosystems*: Berlin, Springer, p. 124-138.
- Ulses, C., Estournel, C., Madron, X.D.d., and Palanques, A., 2008, Suspended sediment transport in the Gulf of Liona (NW Mediterranean): Impact of extreme storms and floods: *Continental Shelf Research*, v. 28, p. 2048-2070.

8. Appendix

Table A1. Total standing stocks (TSS) and average living depths (ALD) for all the benthic foraminifera species identified in this study as well as for the four large benthic foraminifera groups. Totals per station, totals for canyon and slope environments, and overall totals for the whole study area are indicated.

	Canyon								Slope						Total						
	52-C		50-C		47-C		48-C		Total canyon		54-S		51-S		49-S		Total slope		TSS	ALD	
	TSS	ALD	TSS	ALD	TSS	ALD	TSS	ALD	TSS	ALD	TSS	ALD	TSS	ALD	TSS	ALD	TSS	ALD			
<i>Ammobaculites agglutinans</i>								0										2		2	
<i>Ammodiscus anguillae</i>								2					6	1.79				6	1.79	8	1.79
<i>Ammodiscus tenuis</i>								1					2					2		3	
<i>Ammolagena clavata</i>			9	0.36	7	0.54	1	17	0.45	1		5	0.45	13	0.58			19	0.51	36	0.48
<i>Ammonia tepida</i>	5	0.90						5	0.90									0		5	0.90
<i>Ammoscalaria pseudospiralis</i>	118	2.46						118	2.46	4	2.13							4	2.13	122	2.29
<i>Ammoscalaria tenuimargo</i>	13	3.96	3	1.75	1			17	2.86	5	2.65	2		1				8	2.65	25	2.75
<i>Ammosphaeroidina sphaeroidiniformis</i>								0				1						1		1	
<i>Amphicyrina scalaris</i>	6	0.33						6	0.33	15	0.60							15	0.60	21	0.47
<i>Astacolus crepidulus</i>	1							1										0		1	
<i>Bathysiphon capillare</i>								0		1								1		1	
<i>Bathysiphon filiformis</i>								0				1						1		1	
<i>Bathysiphon rufus</i>								0										0		0	
<i>Bathysiphon</i> sp. (smooth)								0										0		0	
<i>Bigenerina cylindrica</i>	11	0.77	2					13	0.77	29	1.46							29	1.46	42	1.11
<i>Bigenerina nodosaria</i>	35	2.34	3	1.33	1			39	1.83	11	1.42							11	1.42	50	1.63
<i>Biloculinella elongata</i>	1							1		11	4.14							11	4.14	12	4.14
<i>Biloculinella globula</i>	2		1		1			0				2						2		2	
<i>Biloculinella labiata</i>							1	1		1		1		1				3		4	
<i>Bolivina alata</i>	1		1					2										0		2	
<i>Bolivina subaenariensis</i> var. <i>mexicana</i>								0		1								1		1	
<i>Botellina labyrinthica</i>								0										0		0	
<i>Bulimina aculeata</i>	42	2.77	2					44	2.77	41	0.66							41	0.66	85	1.72
<i>Bulimina costata</i>	4	0.25	1					5	0.25	1		1						2		7	0.25
<i>Bulimina elongata</i>	9	2.64	4	3.00				13	2.82	6	1.54							6	1.54	19	2.18
<i>Bulimina inflata</i>			1					1		5	0.45							5	0.45	6	0.45
<i>Bulimina marginata</i>	2							2		3	1.50							3	1.50	5	1.50
<i>Cancris auriculus</i>	1							0										0		0	
<i>Cassidulina crassa</i>	3	0.42						3	0.42	1								1		4	0.42
<i>Cassidulina laevigata</i>	1							1										0		1	
<i>Chilostomella oolina</i>	4	1.88	3	2.50				7	2.19	4	3.19							4	3.19	11	2.69
<i>Cibicides kullenbergi</i>			1					1				3	0.42					3	0.42	4	0.42
<i>Cibicides lobatulus</i>	4	0.25						4	0.25	1								0		4	0.25
<i>Cibicides pseudoungeri</i> <i>aunus</i>	1	3.10						1	3.10									0		1	3.10
<i>Cibicides</i> sp.								0		1								1		1	
<i>Cibicides ungerianus</i>	78	1.46	1					2	1.46									0		2	1.46
<i>Cibicides wuellerstorfi</i>								0		1								1		1	
<i>Clavulina multicaemata</i>	2		1					3		3	1.92	3	1.50					6	1.71	9	1.71
<i>Cornuspira carinata</i>								0										0		0	
<i>Cornuspira involvens</i>			1					1										0		1	
<i>Cribostomoides subglobosus</i>								1						1				1		2	
<i>Crithionina</i> cf. <i>C. mamilla</i>	2		21	0.27			1	24	0.27					1				1		25	0.27
<i>Crithionina hispida</i>					2			2										0		2	
<i>Cruciolulina</i> cf. <i>C. triangularis</i>			3	0.25	5	1.10	1	9	0.68			2		2				4		13	0.68
<i>Dendrophyra</i> sp.			1					1										0		1	
<i>Discammina compressa</i>			8	0.56				8	0.56			5	2.20					5	2.20	13	1.38
<i>Discarbina</i> sp.					1			1										0		1	
<i>Eggerelloides scaber</i>	3	0.58						1	0.58	17	1.88							17	1.88	18	1.23
<i>Eggerelloides</i> sp.			1					1										0		1	
<i>Fissurina</i> sp. (striae)								0				1						1		1	
<i>Gavelinopsis praegeri</i>								0		1								1		1	
<i>Gavelinopsis translucens</i>	5	1.50						5	1.50									0		5	1.50
<i>Globobulimina pacifica</i>	1	1.45	1					2	1.45	4	0.88							4	0.88	6	1.16
<i>Globocassidulina subglobosa</i>								0										0		0	
<i>Globulina</i> sp.								0										0		0	
<i>Glomospira charoides</i>			9	1.28	3	0.75	12	1.42	24	1.15	12	1.48	8	0.56	1			21	1.02	45	1.08
<i>Glomospira gordialis</i>	2		1					3										0		3	
<i>Glomospira</i> sp. (white)	4	0.25	1		1			17	0.25	1				1				2		19	0.25
<i>Gyroidinoides altiformis</i>					1		1	2		7	0.39	1		1				9	0.39	11	0.39
<i>Gyroidinoides soldanii</i>			6	0.67			4	0.75	10	0.71		1		3	1.00			4	1.00	14	0.85
<i>Hanzawaia boueana</i>	1							1										0		1	
<i>Hanzawaia</i> cf. <i>H. nitidula</i>	1							1										0		1	
<i>Haplophragmoides quadratus</i>								0		1								1		1	
<i>Haplophragmoides</i> sp. (coarse grains)			1		5	0.45	1	7	0.45	2								2		9	0.45
<i>Haplophragmoides</i> sp. (flat)	2							2										0		2	
<i>Haplophragmoides</i> sp. (very coarse)							2	5										0		5	
<i>Hemisphaerammina bradyi</i>								0						1				1		1	
<i>Hoeglundina elegans</i>					2			2		5	0.35	1		1				7	0.35	9	0.35
<i>Hyalinea balthica</i>	2							2		1								1		3	
<i>Hyperammina elongata</i>			3	1.75				3	1.75			5	0.75	1				6	0.75	9	1.25
<i>Hyperammina</i> sp. (flattened)								0										0		0	
<i>Hyperammina</i> sp. (quartz & spines)	1		1					2										0		2	
<i>Hyperammina</i> sp. (soft & creamy)								0										0		0	
<i>Jaculella acuta</i>			1					1										0		1	
<i>Lagena</i> sp.							1	1										0		1	
<i>Lagena striata</i>								118		1								1		119	
<i>Lagenammina atlantica</i>	9	1.39	1					10	1.39	6	1.42							6	1.42	16	1.40
<i>Lagenammina difflugiformis</i>	13	1.62						13	1.62	2								2		15	1.62
<i>Lagenammina fusiformis</i>	17	3.62	3	2.00	1			21	2.81	4	2.50	1						5	2.50	26	2.65

	52-C		50-C		47-C		48-C		Total canyon		54-S		51-S		49-S		Total slope		TSS	ALD
	TSS	ALD	TSS	ALD	TSS	ALD	TSS	ALD	TSS	ALD	TSS	ALD	TSS	ALD	TSS	ALD	TSS	ALD		
<i>Lagenammina</i> sp. (quartz & shells)	3	0.42							3	0.42	23	0.25					23	0.25	26	0.33
<i>Lenticulina gibba</i>									0				1				1		1	
<i>Lenticulina</i> sp.			1						1								0		1	
<i>Lenticulina vortex</i>			1						1								1		2	
<i>Melanus barleeanus</i>	3	0.75	9	0.97					12	0.86	11	0.86	3	1.25			14	1.06	26	0.96
<i>Milialinella subrotunda</i>									0					2			2		2	
<i>Neolenticulina variabilis</i>	2		1						3		2						2		5	
<i>Nodosaria inflexa</i>									0		1						1		1	
<i>Nodosaria</i> sp.									0								0		0	
<i>Nodosaria submaciata</i>									0		2						2		2	
<i>Nodosaria bradyensis</i>									0								0		0	
<i>Nonion fabum</i>									0		1						1		1	
<i>Nonionella turgida</i>									0		1						1		1	
<i>Nouria polymorphinoides</i>	2								2		1						1		3	
<i>Nummoloculina</i> sp.									0						2		2		2	
<i>Planorbulina mediterraneensis</i>	3	1.33							3	1.33							0		3	1.33
<i>Planularia patens</i>									0								0		0	
<i>Polymorphina</i> sp.	2								6								0		6	
<i>Psamosphaera fusca</i>			4	2.50	2				1	2.50	18	3.00	3	0.75			21	1.88	22	2.19
<i>Psamosphaera</i> sp. (incrusting)	2								0				3	0.58	3	0.75	6	0.67	6	0.67
<i>Psamosphaera</i> sp. (white)									0		2						2		4	
<i>Pseudotrochamina</i> sp.									0								0		0	
<i>Pullenia quinqueloba</i>									0						1		1		1	
<i>Pyrgo anomala</i>							1		13								0		13	
<i>Pyrgo depressa</i>			1		2		2		39		1				3	1.67	4	1.67	43	1.67
<i>Pyrgo lucernula</i>									1						1		1		2	
<i>Pyrgo sarsi</i>	1								6								0		6	
<i>Quinqueloculina</i> cf. <i>Q. venusta</i>	18	1.14							18	1.14	3	1.50	1				4	1.50	22	1.32
<i>Quinqueloculina seminulum</i>	4	0.75							4	0.75	5	0.90					5	0.90	9	0.83
<i>Quinqueloculina</i> sp. (waving suture)	1								1								0		1	
<i>Reophax agglutinatus</i>									0						3	0.25	3	0.25	3	0.25
<i>Reophax arayaensis</i>	1		1						2								0		2	
<i>Reophax dentaliniformis</i>	4	4.00							4	4.00	18	1.74					18	1.74	22	2.87
<i>Reophax scorpiorus</i>	5	2.40		2					7	2.40	4	2.19					4	2.19	11	2.29
<i>Reophax</i> sp. (quartz & shell)	3	0.25							3	0.25							0		3	0.25
<i>Reussella spinulosa</i>									0								0		0	
<i>Rhabdammina linearis</i>									1								0		1	
<i>Robertinoides bradyi</i>									0				1				1		1	
<i>Saccamina</i> sp. (white & grooves)	1								1		1						1		2	
<i>Saccamina</i> sp. (white & smooth)	2								2								2		2	
<i>Saccamina sphaerica</i>					2				2				1				1		3	
<i>Saccorhiza ramosa</i>			1						1					1			3		4	
<i>Sagrina</i> sp.			1						1								0		1	
<i>Saidovina karreriana</i>	1								1		1						1		2	
<i>Sigmoidopsis schlumbergeri</i>	23	3.18	2						25	3.18	2	5	0.90				7	0.90	32	2.04
<i>Siphonina bradyana</i>	1								1								0		1	
<i>Siphotextularia caroliniana</i>									0				1				1		1	
<i>Sphaeroidina bulloides</i>	2		1						3				1				1		4	
<i>Sphaerammina ovalis</i>	1		1						1								0		1	
<i>Spirillina</i> sp.	2								2								0		2	
<i>Spiroplectinella</i> cf. <i>S. taiwanica</i>	18	2.57							18	2.57							0		18	2.57
<i>Spiroplectinella sagittula</i>	45	2.21	1						46	2.21	3	1.00					3	1.00	49	1.61
<i>Stomatobina concentrica</i>	1								1								0		1	
<i>Technitella legumen</i>	1								0		2						2		2	
<i>Telammina fragilis</i>									0				1		6	3.13	7	3.13	7	3.13
<i>Textularia agglutinans</i>	38	2.14							38	2.14	14	1.84					14	1.84	52	1.99
<i>Textularia conica</i>	2								2								0		2	
<i>Thalassina vesicularis</i>	1								1		1						1		2	
<i>Triloculina marioni</i>									0								0		0	
<i>Triloculina</i> sp. (alata)			1						1		2						2		3	
<i>Triloculina tricarinata</i>			1						1								0		1	
<i>Triloculinella</i> sp.									0								0		0	
<i>Tritaxis challengerii</i>					1				1				3	0.25	2		5	0.25	6	0.25
<i>Tritaxis fusca</i>			6	0.25					0	0.25					1		1		1	0.25
<i>Trochammina globigeriniformis</i>	2						1		3		1						1		4	
<i>Uvigerina elongatastriata</i>			1						1								0		1	
<i>Uvigerina mediterranea</i>	2		3	0.38					5	0.38	7	0.54	24	0.99			31	0.76	36	0.57
<i>Uvigerina peregrina</i>									0			4	0.94	8	0.59		12	0.77	12	0.77
<i>Uvigerina peregrina</i> var. <i>celtica</i>	1								1		1	0.35		1			2	0.35	3	0.35
<i>Uvigerina phlegheri</i>									0								0		0	
<i>Uvigerina</i> sp.									0						1		1		1	
<i>Veleroninoides scitulus</i>	1	0.58			2		2		0	0.58	1	0.68					2		3	0.68
Agglutinated dome	8	0.38			33	1.70	48	2.95	89	1.67	1		38	3.74	35	2.85	74	3.29	163	2.48
Single chamber agglutinated (brown quartz)	7	1.17							7	1.17							0		7	1.17
Single chamber agglutinated (hyaline quartz)	7	3.25							0	3.25					15	0.50	15	0.50	15	1.88
Single chamber agglutinated (quartz & shells)	3	0.25	3	3.17					6	1.71	2				1	0.30	3	0.30	9	1.00
Hyaline benthic foraminifera	208	1.37	66	1.63	4	1.33	6	0.75	284	1.27	198	0.76	41	0.85	16	1.01	255	0.87	539	1.07
Porcelaneous benthic foraminifera	27	0.63	7	0.70	8	1.03	6	1.40	48	0.94	23	1.38	6	2.41	11	1.65	40	1.81	88	1.37
Agglutinated benthic foraminifera	421	1.42	87	1.49	61	0.64	71	1.07	640	1.15	301	1.36	89	1.58	415	1.00	805	1.31	1445	1.23
Arborescent & tubular benthic foraminifera	1		7						8		1		8		2		11		19	
TOTAL	657	1.39	167	1.48	73	0.81	83	1.13	980	1.20	523	1.10								

Table A2. Taxonomic index to all the benthic foraminifera species identified in this study. For all the species of which a full identification was possible, the source reference of the scientific name is specified. In the cases of synonymy, the name employed in the source reference is indicated after the reference details.

Species	Descriptor	Source reference
<i>Adercotryma glomeratum</i>	(Brady, 1878)	Jones (1994), page 41, plate 34, figures 15-18.
<i>Ammobaculites agglutinans</i>	(d'Orbigny, 1846)	Jones (1994), page 39, plate 32, figures 19-20.
<i>Ammodiscus anguillae</i>	Höglund, 1947	Jones (1994), page 43, plate 38, figures 1, 27, 3.
<i>Ammodiscus tenuis</i>	Brady, 1881	Jones (1994), page 43, plate 38, figures 4-6.
<i>Ammolagena clavata</i>	(Jones & Parker, 1860)	Jones (1994), page 46, plate 41, figures 12-16.
<i>Ammonia tepida</i>	(Cushman, 1926)	Cimerman and Langer (1991), page 76, plate 87, figures 10-12.
<i>Ammoscalaria pseudospiralis</i>	(Williamson, 1858)	Jones (1994), page 39, plate 33, figures 1-4.
<i>Ammoscalaria tenuimargo</i>	(Brady, 1882)	Jones (1994), page 40, plate 33, figures 13-16.
<i>Ammosphaeroidina sphaeroidiniformis</i>	(Brady, 1884)	Loeblich and Tappan (1988), page 81, plate 67, figures 13-16.
<i>Amphicoryna scalaris</i>	(Batsch, 1791)	Cimerman and Langer (1991), page 52, plate 54, figures 1-9.
<i>Articuluna</i> sp.		
<i>Astacolus crepidulus</i>	(Fichtel & Moll, 1798)	Cimerman and Langer (1991), page 52, plate 54, figures 10-14.
<i>Astrononion</i> sp.		
<i>Bathysiphon capillare</i>	de Folin, 1886	Gooday (1988), page 74, figures 2-5.
<i>Bathysiphon filiformis</i>	M. Sars, 1871	Gooday (1988) page 97, figures 1-3.
<i>Bathysiphon rufus</i>	de Folin, 1886	Gooday (1988), page 84, figures 12-14.
<i>Bathysiphon</i> sp. (smooth)		
<i>Bigenerina cylindrica</i>	Cushman, 1922	Jones (1994), page 49, plate 44, figures 19-24.
<i>Bigenerina nodosaria</i>	d'Orbigny, 1826	Jones (1994), page 49, plate 44, figures 14-18.
<i>Biloculinella elongata</i>	(Wiesner, 1923)	Cimerman and Langer (1991), page 39, plate 36, figures 3-4.
<i>Biloculinella globula</i>	(Bornemann, 1855)	Cimerman and Langer (1991), page 40, plate 36, figures 1-2.
<i>Biloculinella labiata</i>	(Schlumberger, 1891)	Cimerman and Langer (1991), page 40, plate 36, figure 12.
<i>Bolivina alata</i>	(Seguenza, 1862)	Cimerman and Langer (1991), page 59, plate 61, figures 12-14 (As: <i>Brizalina alata</i>).
<i>Bolivina dilatata</i>	Reuss, 1850	Cimerman and Langer (1991), page 59, plate 62, figure 2 (As: <i>Brizalina dilatata</i>).
<i>Bolivina</i> sp.		
<i>Bolivina spathulata</i>	(Williamson, 1858)	Cimerman and Langer (1991), page 60, plate 62, figures 3-5 (As: <i>Brizalina spathulata</i>).
<i>Bolivina striatula</i>	Cushman, 1922	Cimerman and Langer (1991), page 60, plate 62, figures 6-9 (As: <i>Brizalina striatula</i>).
<i>Bolivina subaenariensis</i> var. <i>mexicana</i>	Cushman, 1922	Jones (1994), page 58, plate 53, figures 10-11 (As: <i>Brizalina subaenariensis</i> var. <i>mexicana</i>)
<i>Botellina labyrinthica</i>	Brady, 1881	Jones (1994), page 36, plate 29, figures 8-18.
<i>Bulimina aculeata</i>	d'Orbigny, 1826	Cimerman and Langer (1991), page 61, plate 63, figures 10-11.
<i>Bulimina costata</i>	d'Orbigny, 1852	Mojtahid et al. (2006), plate 1, figure 7.
<i>Bulimina elongata</i>	d'Orbigny, 1826	Cimerman and Langer (1991), page 62, plate 64, figures 3-8.
<i>Bulimina inflata</i>	Seguenza, 1862	Timm (1992), plate 5, figure 10.
<i>Bulimina marginata</i>	d'Orbigny, 1826	Cimerman and Langer (1991), page 62, plate 64, figures 9-11.
<i>Cancris auriculus</i>	(Fichtel & Moll, 1798)	Loeblich and Tappan (1988), page 545, plate 591, figures 1-3.
<i>Cassidulina crassa</i>	d'Orbigny, 1839	Jones (1994), page 60, plate 54, figure 4.
<i>Cassidulina laevigata</i>	d'Orbigny, 1826	Cimerman and Langer (1991), page 61, plate 63, figures 1-3.
<i>Cassidulinoides</i> cf. <i>C. bradyi</i>	Cushman, 1922	Jones (1994), page 60, plate 54, figures 6-9 (For: <i>Cassidulinoides bradyi</i>)
<i>Chilostomella oolina</i>	Schwager, 1878	Jones (1994), page 61, plate 55, figures 12-14, 17-18.
<i>Cibicides kullenbergi</i>	Parker, 1953	Schweizer (2006), page 124, plate 4, figures a-m.
<i>Cibicides lobatulus</i>	(Walker & Jacob, 1798)	Schweizer (2006), page 124, plate 5, figures a-l.
<i>Cibicides pseudoungerianus</i>	(Cushman 1922)	Schweizer (2006), page 125, plate 7, figures a-p.
<i>Cibicides</i> sp.		
<i>Cibicides ungerianus</i>	(d'Orbigny, 1846)	Schweizer (2006), page 127, plate 10, figures a-m.
<i>Cibicides wuellerstorfi</i>	(Schwager, 1866)	Schweizer (2006), page 127, plate 11, figures a-l.
<i>Clavulina multicamerata</i>	Chapman, 1907	Jones (1994), page 53, plate 48, figures 17-18.
<i>Cornuspira carinata</i>	(Costa, 1856)	Jones (1994), page 27, plate 11, figure 4.
<i>Cornuspira involvens</i>	(Reuss, 1850)	Jones (1994), page 26, plate 11, figures 1-3.
<i>Cribostomoides subglobosus</i>	(Cushman, 1910)	Jones (1994), page 40, plate 34, figures 8-10.
<i>Crithionina</i> cf. <i>C. mamilla</i>	Goes, 1894	Loeblich and Tappan (1988), page 38, plate 28, figures 1-4 (For: <i>Crithionina mamilla</i>).
<i>Crithionina hispida</i>	Flint, 1899	Koho (2007), page 43, plate 2, figure 2.
<i>Crithionina</i> sp. (shell)		
<i>Cruciloculina</i> cf. <i>C. triangularis</i>	d'Orbigny, 1826	Loeblich and Tappan (1988), page 338, plate 347, figures 8-12. (As: <i>Cruciloculina triangularis</i>)
<i>Dendrprhya</i> sp.		
<i>Discammina compressa</i>	(Goes, 1882)	Jones (1994), page 40, plate 33, figures 26-28.
<i>Discorbina</i> sp.		
<i>Eggerelloides scaber</i>	(Williamson, 1858)	Cimerman and Langer (1991), page 21, plate 8, figure 7 (As: <i>Eggerelloides scabrus</i>)
<i>Eggerelloides</i> sp.		
<i>Elphidium</i> cf. <i>E. advenum</i>	(Cushman, 1922)	Cimerman and Langer (1991), page 77, plate 89, figures 5-7 (As: <i>Elphidium</i> cf. <i>E. advenum</i>)
<i>Epistominella</i> sp.		
<i>Eponides pusillus</i>	Parr, 1950	Gooday and Hughes (2002), page 105, plate 1, figures i-k.
<i>Fissurina cucullata</i>	Silvestri, 1902	Jones (1994), page 68, plate 59, figure 25.
<i>Fissurina</i> sp. (striae)		
<i>Fissurina staphyllearia</i>	(Schwager, 1866)	Jones (1994), page 67, plate 59, figures 8-11.
<i>Gavelinopsis praegeri</i>	(Heron-Allen & Earland, 1913)	Cimerman and Langer (1991), page 66, plate 70, figures 3-4.
<i>Gavelinopsis translucens</i>	(Phleger & Parker, 1951)	Schiebel (1992), plate 4, figure 5.
<i>Globbulimina pacifica</i>	Cushman, 1927	Jones (1994), page 54, plate 50, figures 7-10.
<i>Globocassidulina subglobosa</i>	(Brady, 1881)	Cimerman and Langer (1991), page 61, plate 63, figures 4-6.
<i>Globulina</i> sp.		
<i>Glomospira charoides</i>	Jones & Parker, 1860	Cimerman and Langer (1991), page 17, plate 3, figures 6-9 (As: <i>Repmania charoides</i>).
<i>Glomospira gordialis</i>	(Jones & Parker 1860)	Cimerman and Langer (1991), page 17, plate 3, figures 4-5.
<i>Glomospira</i> sp. (white)		
<i>Gyroidinoides altiformis</i>	Stewart and Stewart	Narayan et al. (2005), page 130, plate 4, figures 1-2.
<i>Gyroidinoides soldanii</i>	(d'Orbigny, 1826)	Cimerman and Langer (1991), page 75, plate 85, figures 5-6.
<i>Gyroidinoides umbonatus</i>	(Silvestri, 1898)	
<i>Hanzawaia boueana</i>	(d'Orbigny)	
<i>Hanzawaia</i> cf. <i>H. nitidula</i>	(Bandy)	
<i>Haplophragmoides quadratus</i>	Earland, 1934	
<i>Haplophragmoides</i> sp. (coarse grains)		

<i>Haplophragmoides</i> sp. (flat)		Cimerman and Langer (1991), page 18, plate 4, figure 10 (As: <i>Haplophragmoides</i> sp.).
<i>Haplophragmoides</i> sp. (smooth & globular)		
<i>Haplophragmoides</i> sp. (very coarse)		
<i>Hemisphaerammina bradyi</i>	Loeblich & Tappan, 1957	Jones (1994), page 46, plate 41, figure 11.
<i>Hoeglundina elegans</i>	(d'Orbigny, 1826)	Cimerman and Langer (1991), page 70, plate 74, figures 4,7, 75-6
<i>Hormosinella guttifer</i>	(Brady, 1881)	Jones (1994), page 38, plate 31, figures 10-15.
<i>Hyalinea balthica</i>	(Schroeter, 1783)	Jones (1994), page 110, plate 112, figure 1-2.
<i>Hyperammina elongata</i>		
<i>Hyperammina</i> sp. (flattened)		
<i>Hyperammina</i> sp. (quartz & spines)		
<i>Hyperammina</i> sp. (soft & creamy)		
<i>Jaculella acuta</i>	Brady, 1879	Jones (1994), page 33, plate 22, figure 14-18.
<i>Lagena</i> sp.		
<i>Lagena striata</i>	(d'Orbigny, 1839)	Cimerman and Langer (1991), page 53, plate 55, figures 6-7.
<i>Lagenammina atlantica</i>	(Cushman, 1944)	Cimerman and Langer (1991), page 15, plate 1, figures 1-3.
<i>Lagenammina difflugiformis</i>	(Brady, 1879)	Jones (1994), page 36, plate 30, figures 1-3.
<i>Lagenammina fusiformis</i>	(Williamson, 1858)	Cimerman and Langer (1991), page 15, plate 1, figures 4-5.
<i>Lagenammina</i> sp. (organic wall)		
<i>Lagenammina</i> sp. (quartz & shells)		
<i>Lagenammina tubulata</i>	Rhumbler, 1931	Timm (1992), plate 1, figure 14 (As: <i>Reophax tubulatum</i>)
<i>Lenticulina gibba</i>	(d'Orbigny, 1826)	Cimerman and Langer (1991), page 51, plate 53, figures 7-11.
<i>Lenticulina</i> sp.		
<i>Lenticulina vortex</i>	(Fichtel & Moll, 1798)	Jones (1994), page 81, plate 69, figures 14-16.
<i>Melonis barleeanus</i>	(Williamson, 1858)	Loeblich and Tappan (1988), page 621, plate 696, figures 5-6. (As: <i>Melonis barleeaanum</i>)
<i>Miliolinella subrotunda</i>	(Montague, 1803)	Cimerman and Langer (1991), page 42, plate 38, figures 4-9.
<i>Neolenticulina variabilis</i>	(Reuss, 1850)	Jones (1994), page 80, plate 68, figures 11-16.
<i>Nodosaria inflexa</i>	Reuss, 1866	Cimerman and Langer (1991), page 51, plate 52, figures 4-6 (As: <i>Laevidentalina inflexa</i>).
<i>Nodosaria</i> sp.		
<i>Nodosaria subemaciata</i>	(Parr, 1950)	Jones (1994), page 74, plate 62, figures 25-26 (As: <i>Dentalina subemaciata</i>)
<i>Nodosaria bradyensis</i>	(Dervieux, 1894)	Jones (1994), page 73, plate 62, figures 19-20 (As: <i>Dentalina bradyensis</i>)
<i>Nonion fabum</i>	(Fichtel & Moll, 1798)	Jones (1994), page 108, plate 109, figures 12-13.
<i>Nonion</i> sp.		
<i>Nonionella turgida</i>	(Williamson, 1858)	Jones (1994), page 108, plate 109, figures 17-19.
<i>Nouria polymorphinoides</i>	Heron-Allen & Earland, 1914	Cimerman and Langer (1991), page 20, plate 7, figures 1-3.
<i>Nummoloculina</i> sp.		Cimerman and Langer (1991), page 47, plate 44, figures 9-11 (As: <i>Nummoloculina</i> sp.)
<i>Pesudoparella</i> sp.		
<i>Planorbulina mediterraneensis</i>	d'Orbigny, 1826	Cimerman and Langer (1991), page 71, plate 78, figures 1-8.
<i>Planularia patens</i>	(Brady, 1884)	Jones (1994), page 79, plate 67, figures 15-16.
<i>Polymorphina</i> sp.		
<i>Psamosphaera fusca</i>	Schulze, 1875	Jones (1994), page 31, plate 18, figures 1-8.
<i>Psamosphaera</i> sp. (incrusting)		
<i>Psamosphaera</i> sp. (white)		
<i>Pseudotrochamina</i> sp.		
<i>Pullenia quinqueloba</i>	(Reuss, 1851)	Jones (1994), page 92, plate 84, figures 14-15.
<i>Pyrgo anomala</i>	(Schlumberger, 1891)	Cimerman and Langer (1991), page 44, plate 41, figures 3-5.
<i>Pyrgo depressa</i>	(d'Orbigny, 1826)	Jones (1994), page 19, plate 2, figures 12, 16-17.
<i>Pyrgo lucernula</i>	(Schwager, 1891)	Cimerman and Langer (1991), page 45, plate 41, figures 10-11.
<i>Pyrgo sarsi</i>	(Schlumberger, 1891)	Jones (1994), page 18, plate 2, figure 7.
<i>Quinqueloculina</i> cf. <i>Q. venusta</i>	Karrer, 1868	Jones (1994), page 21, plate 5, figure 7 (For: <i>Quinqueloculina venusta</i>)
<i>Quinqueloculina schlumbergeri</i>	(Wiesner, 1923)	Schiebel (1992), plate 5, figure 6.
<i>Quinqueloculina seminulum</i>	(Linnaeus, 1758)	Cimerman and Langer (1991), page 38, plate 34, figures 9-12. (As: <i>Quinqueloculina seminula</i>).
<i>Quinqueloculina</i> sp.		
<i>Quinqueloculina</i> sp. (waving suture)		
<i>Reophax agglutinatus</i>	Cushman, 1913	Jones (1994), page 37, plate 30, figure 13.
<i>Reophax arayaensis</i>	Bermúdez and Seiglie, 1963	Elis and Messina (1940), supplement for 1972, no. 1.
<i>Reophax dentaliniformis</i>	Brady, 1881	Jones (1994), page 37, plate 30, figures 21-22.
<i>Reophax scorpiorus</i>	Montfort, 1808	Cimerman and Langer (1991), page 17, plate 4, figures 1-4.
<i>Reophax</i> sp. (pointy chamber)		
<i>Reophax</i> sp. (quartz & shell)		
<i>Reophax</i> sp. (shell plates)		
<i>Reussella spinulosa</i>	(Reuss, 1850)	Cimerman and Langer (1991), page 63, plate 66, figures 5-8.
<i>Rhabdammina linearis</i>	Brady, 1879	Jones (1994), page 32, plate 22, figures 1-3.
<i>Robertinoidea bradyi</i>	(Cushman & Parker, 1936)	Jones (1994), page 55, plate 50, figure 18.
<i>Rosalina bradyi</i>	(Cushman, 1915)	Cimerman and Langer (1991), page 66, plate 71, figures 1-5.
<i>Saccammina</i> sp. (white & grooves)		
<i>Saccammina</i> sp. (white & smooth)		
<i>Saccammina sphaerica</i>	M. Sars, 1868	Jones (1994), page 31, plate 18, figures 11-15, 17?
<i>Saccorhiza ramosa</i>	(Brady, 1879)	Cimerman and Langer (1991), page 16, plate 2, figures 4-5.
<i>Sagrina</i> sp.		
<i>Saidovina karrieriana</i>	(Brady, 1881)	Jones (1994), page 59, plate 53, figures 19-21.
<i>Sigmallinita tenuis</i>	(Czjzek, 1848)	Cimerman and Langer (1991), page 48, plate 45, figures 7-10.
<i>Sigmallopsis schlumbergeri</i>	(Silvestri, 1904)	Cimerman and Langer (1991) page 48, plate 46, figures 10-14.
<i>Siphonina bradyana</i>	Cushman, 1927	Jones (1994), page 100, plate 96, figure 8.
<i>Siphotextularia caroliniana</i>		
<i>Sphaeroidina bulloides</i>	(d'Orbigny, 1826)	Jones (1994), page 91, plate 84, figures 1-5, 6-7?
<i>Sphaerammina ovalis</i>	Cushman, 1910	Loeblich and Tappan (1988), page 69, plate 52, figures 8-12.
<i>Spirillina</i> sp.		
<i>Spiroplectinella</i> cf. <i>S. taiwanica</i>	(Chang, 1956)	Cimerman and Langer (1991), page 19, plate 6, figures 7-9 (As: <i>Spiroplectinella</i> cf. <i>S. taiwanica</i>).
<i>Spiroplectinella sagittula</i>	(d'Orbigny, 1839)	Cimerman and Langer (1991), page 19, plate 6, figures 5-6.
<i>Stomatobina concentrica</i>	Parker & Jones, 1864	Cimerman and Langer 1991, page 65, plate 68, figures 7-9.

<i>Technitella legumen</i>	Norman, 1878	Cimerman and Langer (1991), page 15, plate 1, figures 6-7.
<i>Telammina fragilis</i>	Goody & Haynes, 1983	Loeblich and Tappan (1988), page 56, plate 43, figures 8-11.
<i>Textularia agglutinans</i>	d'Orbigny, 1839	Cimerman and Langer (1991), page 21, plate 10, figures 1-2.
<i>Textularia conica</i>	(d'Orbigny, 1839)	Cimerman and Langer (1991), page 22, plate 10, figures 7-9.
<i>Thalosisa vesicularis</i>	(Brady, 1879)	Jones (1994), page 42, plate 35, figures 18-19.
<i>Triloculina marioni</i>	Schlumberger, 1893	Cimerman and Langer (1991), page 46, plate 43, figures 1-5.
<i>Triloculina</i> sp. (alata)		
<i>Triloculina tricarinata</i>	d'Orbigny, 1826	Cimerman and Langer (1991), page 46, plate 44, figures 3-4.
<i>Triloculinella</i> sp.		
<i>Tritaxis challengerii</i>	(Hedley, Hurdle & Burdett, 1964)	Jones (1994), page 46, plate 41, figure 3.
<i>Tritaxis fusca</i>	(Williamson, 1858)	Jones (1994), page 54, plate 49, figure 13.
<i>Trochammina globigeriniformis</i>	Parker & Jones, 1865	Cimerman and Langer (1991), page 20, plate 7, figures 4-6 (As: <i>Ammoglobigerina globigeriniformis</i>).
<i>Trochammina</i> sp. (flat)		
<i>Trochammina</i> sp. (globular)		
<i>Uvigerina elongatastriata</i>	(Colom, 1952)	Schweizer (2006), page 130, plate 15, figures a-q.
<i>Uvigerina mediterranea</i>	Hofker, 1932	Schweizer (2006), page 131, plate 16, figures a-p.
<i>Uvigerina peregrina</i>	Cushman, 1923	Schweizer (2006), page 131, plate 17, figures a-p.
<i>Uvigerina peregrina</i> var. <i>celtica</i>		Koho (2008), page 64, plate 1, figure 3.
<i>Uvigerina phlegherii</i>	Le Calvez, 1959	Schweizer (2006), page, 132, plate 18, figures a-x.
<i>Uvigerina</i> sp.		
<i>Veleroninoides scitulus</i>	(Brady, 1881)	Jones (1994), page 41, plate 34, figures 11-13.
Agglutinated dome		
Single chamber agglutinated (brown quartz)		
Single chamber agglutinated (hyaline quartz)		
Single chamber agglutinated (mica)		
Single chamber agglutinated (quartz & shells)		
